



Project acronym: **LASH FIRE**  
Project full title: **Legislative Assessment for Safety Hazard of Fire and Innovations in Ro-ro ship Environment**  
Grant Agreement No: **814975**  
Coordinator: **RISE Research Institutes of Sweden**



## **Deliverable D08.11**

# **Description of prototypes and demonstration for identification of vehicles and ignition sources**

**August 2023**

Dissemination level: **Public**

## Abstract

Two systems have been developed to perform detection of potential ignition sources and identify vehicles on shore and on board ships. The main purpose of the Vehicle Hot Spot Detection (VHD) system located on shore is to prevent vehicles with abnormal temperature readings from boarding the ship and be lead away for inspection at an early stage. The Automated Guided Vehicle (AGV), on the other hand, has the main purpose of continuously scanning the cargo space of the ship for temperature anomalies that occur during the voyage.

The AGV is based on a set of sensors containing LiDAR, RGB camera and thermal camera. Based on these inputs it is intended to navigate, detect license plates and detect thermal hotspots. The VHD system is built as a stationary gate that processes the license plates and temperature information of the vehicles passing through.

These systems should be considered parts of a systems of systems approach where a single system struggles to achieve a sufficient coverage both on shore and offshore. This report covers the design of these systems, design choices made and discussion of experiences gained during designing and demonstarations of the systems.



*This project has received funding from the European Union's Horizon 2020 research and innovation programme under grant agreement No 814975*

*The information contained in this deliverable reflects only the view(s) of the author(s). The Agency (CINEA) is not responsible for any use that may be made of the information it contains.*

The information contained in this report is subject to change without notice and should not be construed as a commitment by any members of the LASH FIRE consortium. In the event of any software or algorithms being described in this report, the LASH FIRE consortium assumes no responsibility for the use or inability to use any of its software or algorithms. The information is provided without any warranty of any kind and the LASH FIRE consortium expressly disclaims all implied warranties, including but not limited to the implied warranties of merchantability and fitness for a particular use.

© COPYRIGHT 2019 The LASH FIRE Consortium

This document may not be copied, reproduced, or modified in whole or in part for any purpose without written permission from the LASH FIRE consortium. In addition, to such written permission to copy, acknowledgement of the authors of the document and all applicable portions of the copyright notice must be clearly referenced. All rights reserved.

## Document data

Document Title:	D08.11 - Description of prototypes and demonstration for identification of vehicles and ignition sources		
Work Package:	WP08 – Ignition		
Related Task(s):	T08.7, T08.8		
Dissemination level:	Public		
Deliverable type:	Report		
Lead beneficiary:	1 – RISE		
Responsible author:	Robert Rylander		
Co-authors:	Martin Torstensson, Leon Sütfeld, Maria Ulan, Joakim Rosell, Max Fransson, Lukas Wallimann		
Date of delivery:	2023-08-15		
References:	D08.1, D04.1, D08.9, D08.10		
Approved by	Francisco Rodero CIM on 2023-08-15	Hedvig Aminoff NTNU on 2023-08-15	Maria Hjohlman, RISE on 2023-08-15

## Involved partners

No.	Short name	Full name of Partner	Name and contact info of persons involved
01	RISE	RISE Research Institutes of Sweden AB	Robert Rylander, Robert.rylander@ri.se
02	SICK	SICK AG	Lukas Wallimann, lukas.wallimann@sick.ch

## Document history

Version	Date	Prepared by	Description
01	2021-09-10	Robert Rylander	Draft of structure
02	2023-03-28	Robert Rylander	Draft of final report
03	2023-06-19	Robert Rylander	Reviewed draft of final report
04	2023-08-15	Robert Rylander	Final version

## Content

1	Executive summary .....	7
1.1	Problem definition.....	7
1.2	Methods .....	7
1.3	Results and achievements.....	8
1.4	Contribution to LASH FIRE objectives.....	8
1.5	Exploitation and implementation.....	8
2	List of symbols and abbreviations .....	10
3	Introduction.....	11
3.1	Purpose.....	11
3.2	Solution.....	11
3.3	Challenges.....	11
4	Vehicle hotspot detection .....	12
4.1	Description .....	12
4.2	Research and development of a LASH FIRE VHD system .....	13
	Using LWIR sensors to create a heat map of each side of the object. ....	21
	Final choices of software .....	21
	Cameras for reading license plates and ADR/DG placards.....	22
	ADR/DG placard readers .....	25
	System of systems .....	27
4.3	Finding and segmenting the refrigeration units using machine learning. ....	28
	The sensors installed for thermographic profiling at Majnabbe.....	28
5	Analysis of thermal sensor data collected.....	33
6	Usage of machine learning to find refrigeration units. ....	35
6.1	Results from the demonstrator at Majnabbe .....	35
	When a VHD alarm is raised in the VHD System .....	35
7	Automated Guided Vehicle .....	39
7.1	Final choices of hardware .....	39
7.1.1	Chassis .....	39
7.1.2	Batteries .....	39
7.1.3	LiDAR .....	39
7.1.4	Camera RGB.....	40
7.1.5	Processing unit .....	40
7.1.6	Thermal Camera .....	40
7.2	AGV 3D model .....	44

7.3	Final choices of software .....	46
	Mapping.....	47
	Calibration .....	49
	Navigation and path planning .....	50
	Path following / locomotion.....	51
	Collision avoidance .....	52
	License plate detection .....	52
	Hot spot detection.....	52
8	AGV test and demonstration.....	52
8.1	Functional requirements and tests.....	52
	Test design.....	52
	Scenario description .....	53
8.2	Test results.....	55
	T1.1 - PID motor control isolated.....	55
	T2.1 - Collision avoidance for dynamic obstacles (lab test) .....	56
	T2.2 - Navigation in lab environment.....	56
	<b>T2.3 Vehicle identification in lab environment</b> .....	57
	T3.1 - Navigation in relevant environment .....	60
	T3.2 - Temperature readout and license plate detection in relevant environment.....	64
	T3.3 - Combined navigation, temperature readout, and license plate detection in relevant environment .....	65
	T4.1 - Battery runtime test .....	65
9	Discussion .....	66
9.1	VHD.....	66
9.2	License plate detection .....	66
	Normal operation temperature baseline on refrigeration units .....	67
9.3	AGV.....	67
	LiDAR .....	67
	Computer Hardware.....	68
	Motor controller .....	69
	Batteries .....	69
	Code performance optimization .....	69
	License plate detection .....	70
	Improved SLAM precision through odometry and IMU.....	70
	Communication with external devices.....	71
	Thermal cameras .....	71

System of systems .....	71
10 Conclusion .....	72
11 References.....	73
12 Indexes .....	75
12.1 Index of tables .....	75
12.2 Index of figures.....	75
13 ANNEXES.....	77
13.1 ANNEX A Highest 100 recorded refrigeration units .....	77
13.2 ANNEX B Plots of LWIR temperature readings.....	80
13.3 ANNEX C Most used temperature settings in VHD systems .....	82

# 1 Executive summary

## 1.1 Problem definition

The majority of fires on ro-ro ships start in the cargo itself due to many different reasons. In the D08.01 Definition and parametrization of critical fire hazards, classification of cargoes, transport units, engines, fuels and vessels and identification methodologies [1] the background and scope for the work done is described. This report aims to investigate the possibilities of using Automated Guided Vehicles (AGVs) and Vehicle Hotspot Detectors (VHDs) to detect potential ignition sources. The first by patrolling the cargo deck after the loading is completed and the second to scan vehicles before boarding. Infrared sensors are used to monitor the cargo and detect heat anomalies e.g., hot spots directly or over time on the undercarriage of the cargo. The usage of AGVs allows for a continuous presence at the cargo deck, filling the gaps between the ship crew's fire patrols.

The scope for the AGV originated from continuous monitoring of BEVs that could be allowed to be charged during a sea passage in addition to specific areas, cargoes and units of specific interest e.g., dangerous goods or cargo that possess an elevated risk but are allowed onboard the ship.

## 1.2 Methods

Proof-of-concept systems has been constructed, to identify potential ignition sources in addition to finding abnormal heat levels in cargo and transports during shipping. The proposed solution is to utilize a combination of two different systems.

The first is a stationary VHD system located onshore before the loading of the ship. At this point a vehicle or cargo with a detected heat anomaly can be diverted away from other transports at the terminal and either investigated at some specified location or kept from being loaded on ship.

The second is an AGV operating on the ship, the aim over time is not to replace manual inspections of the cargo but complement and enhance them with patrolling automated drones. However, for the foreseeable future these systems will be acting as a supplement to the crew's inspections and over time increase vigilance of the overall monitoring of the cargo areas. The drones will be scanning for abnormal heat levels.

### **AGV (Automated Guide Vehicle)**

The suggested approach for performing the mobile screening of cargo is based on an AGV. For the drone to be able to navigate and avoid colliding with objects it needs sensors for detecting where it is and what to avoid. The two major tasks for the AGV are to create a map covering potential fire hazards and to patrol these to detect if a heat anomaly occurs. To achieve these goals some of the technical challenges that need to be addressed are navigation, path planning, collision avoidance and object detection. The path planning is required to create a functional route for the drone to take in a changing environment where it cannot be guaranteed that the same path will be the most efficient or even possible. For the path planning to have any significance it is also important to have a system of navigation both for the drone to localize itself but also to detect and track obstacles and cargo to monitor. While the drone is moving it will likely meet several obstacles on its way. Therefore, collision avoidance is a necessary functionality to avoid crashes. With the goal of finding potential ignition sources, object detection is applied by detection of license plates.

D08.01 Definition and parametrization of critical fire hazards, classification of cargoes, transport units, engines, fuels and vessels and identification methodologies [1] provides information on the challenges and requirements of the solution, giving important background information. In D04.01 Review of accident causes and hazard identification report [2] information of potential ignition sources has been provided. Finally, D08.09 Prototyping and demonstration of vehicle identification



tool [3] and D08.10 Demonstration of prototype for detection of potential ignition sources [4] cover the demonstrators for object detection and ignition source detection respectively.

### **VHD (Vehicle Hot Spot Detector)**

The stationary VHD system architecture and components are described in D08.1 [1] The demonstration [3],[4] is built upon SICK AG's Vehicle Hotspot Detection (VHD) system. It uses high precision LiDAR for positioning, measuring, and profiling of the vehicle. It has Long Wave Infrared (LWIR) sensors for thermographic profiling of the vehicle.

To be able to detect the refrigeration AC unit that is most commonly on the units shipped on ships, located at the front of the vehicle cargo space or the front of the trailer the VHD system needed development of both hardware and software. To the system one LiDAR was added for positioning and tracking of the vehicle as it passes through the system and one LiDAR combined with an additional LWIR sensor for profiling of the topside of the vehicle. To the system was also added a new feature that used two extra Automatic Number Plate Reader (ANPR) that registered the rear license plate and ADR/IMDG placard readers, so both the truck and the trailers could be identified since many trailers are shipped without an accompanied driver.

### 1.3 Results and achievements

Based on result from the demonstrations, it has been validated that it is possible to use a VHD portal to detect and segment out the refrigeration units, this can then trigger an alarm and preventive actions then taken. The first response will vary depending on the organisation, facilities but it can serve well as a first guard against allowing potentially hazardous transports of refrigeration units on to a ship. It is capable of detecting and visualizing heat sources on transports.

The AGV demonstrates a promising approach for continuous heat abnormality checks within the cargo spaces of ships. A proof of concept was created to demonstrate the possibilities of AGVs as a means to scan vehicles temperatures. This also included tests of detection of license plates based on images from an RGB camera and heat detection with a thermal camera mounted to the AGV. In order to achieve this, a navigation system was developed containing path planning, path following, localization, motor heuristics etc.

The results are satisfying and the developed software and hardware for this project has demonstrated that they can be used to fulfill the tasks T08.8 Demonstration of detection of potential ignition sources and T08.7 Demonstration of vehicle identification tool.

### 1.4 Contribution to LASH FIRE objectives

This report covers the description of the development and also the demonstrations of two technical solutions for automatic screening of cargo that WP8-A was intended to create. Regarding the AGV this report details the hardware and software choices for the AGV and also covers the development and evaluation of the demonstrator. For the VHD the modifications of the VHD system aim to improve the understanding of reefer unit's heat signatures and the possibility for early warning of anomalies if detected heat signature is more than accepted maximum temperature threshold. The physical modifications made to the VHD system aim to make it more flexible and investigate how compact/close to a ship it could be installed.

### 1.5 Exploitation and implementation

The system is intended to be used by shipping companies. The mobile system that allows screening of a cargo deck is intended to reduce the risk of fires erupting during the voyage. The information about temperatures and fire hazards in combination with their location could be made available through e.g. the stowage planning system. The VHD system needs to be implemented and

maintained by the ports as it is a part of the infrastructure or installed on the ship as vehicles roll onboard.

## 2 List of symbols and abbreviations

2D	Two Dimensional
3D	Three Dimensional
AC	Air Conditioning unit
ADR	A Accord européen relatif au transport international des marchandises Dangereuses par Route
AFV	Alternative Fuel Vehicle, see APV
AGV	Automated Guided Vehicle
ANPR	Automatic Number Plate Reader
APU	Application-Processing Unit
APV	Alternative Powered Vehicle
BEV	Battery Electric Vehicle
DG	short for Dangerous Goods, see IMDG
IMDG	International Maritime Dangerous Goods Code.
LF	LASH FIRE project
LIDAR	Light Detection and Radar sensor
LPR	License Plate Reader
LWIR	Longwave Infrared
ML	Machine Learning algorithms
Reefer	Refrigeration Unit e.g. air conditioning unit on a trailer or container
RGB	Red Green Blue
VDG	Vehicle Dangerous Goods detection system
VHD	Vehicle Hotspot Detection system
SPT	Stowage Planning Tool
TOS	Terminal Operation System

## 3 Introduction

Main author of the chapter: Martin Torstensson, RISE

### 3.1 Purpose

To prevent fires from starting in vehicles or cargo loaded into a ship an automatic system is proposed. The solution is intended to monitor both cargo, vehicles, and carriers (trailers etc.) to find deviating temperatures in addition to providing information to help identify the location of units of specific interest. This information is to be transmitted to the ship's crew to provide possibilities for fire prevention in time or to know where efforts need to be focused. A summary of different software and hardware solutions is presented. More information on the potential ignition sources can be found in D08.1 Definition and parametrization of critical fire hazards, classification of cargoes, transport units, engines, fuels and vessels and identification methodologies [1] and D04.1 Definition and parametrization of critical fire hazards, classification of cargoes, transport units, engines, fuels and vessels and identification methodologies [2]

### 3.2 Solution

A two-system solution is tested. One stationary system, placed before boarding (VHD) and the other is a mobile system (AGV) operating inside of the ship. When a transport approaches for boarding it can pass under the stationary system making it possible to detect abnormal heat at a time when it is still possible to prevent it from boarding the ship until it has been further investigated. The mobile solution is intended to continuously travel through the cargo hold and measure temperatures. If there is a temperature reading that stands out it can be reported alongside location to the ship's crew for further inspection.

### 3.3 Challenges

There are several conditions specific to the environment of the ship that pose specific challenges for the proposed systems. More information on challenges can be found in D08.1 [1] where these have, for simplicity, been separated into internal and external challenges. Where the internal challenges are e.g., design of the ship's terminal and cargo decks, while the external challenges are those that cannot be controlled, such as the weather.

## 4 Vehicle hotspot detection

Main author of the chapter: Robert Rylander, RISE

### 4.1 Description

To be able to scan as much as possible of a truck, trailer, or cargo for heat anomalies with a minimum intrusion on the object and the flow of units, a portal with fixed sensors, line of sight of the sides and top-down view of the object is used. Illustrated below is a set-up of a VHD with the modifications added by the LASHFIRE project, top-down long wave infrared (LWIR) and one extra LiDAR for high precision longitudinal tracking of the object as it passes the VHD portal.



Figure 1 Illustration of the physical installation of a VHD system (SICK)

The two LiDAR sensors, illustrated sending red light beams below, was a necessity to provide line of sight in the cramped space with minimal head room due to an office building prior to the gate at the Majnabbe terminal.

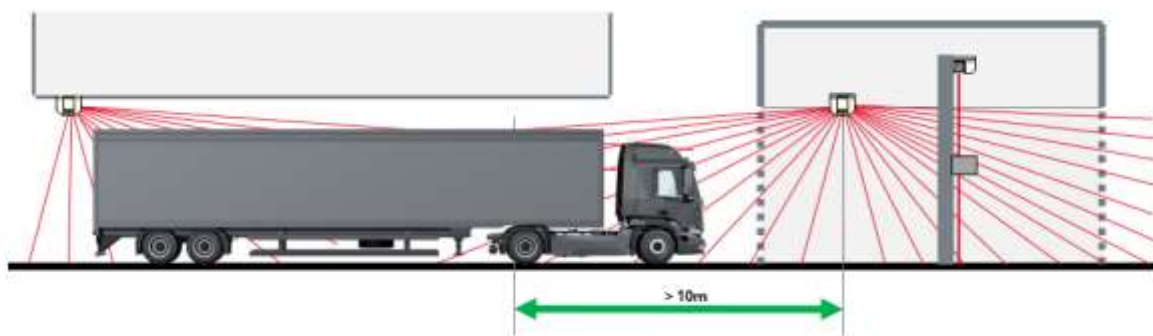


Figure 2 The two LiDARs used for longitudinal tracking of the object. (SICK)

This allowed accurate tracking of the object as it enters and passes through the VHD. This facilitated the high precision measurements of the vehicles, needed for the algorithms in the software to do segmentation of the units into relevant parts and sections. This is used for differential temperature zones and corresponding alarm thresholds as illustrated below.

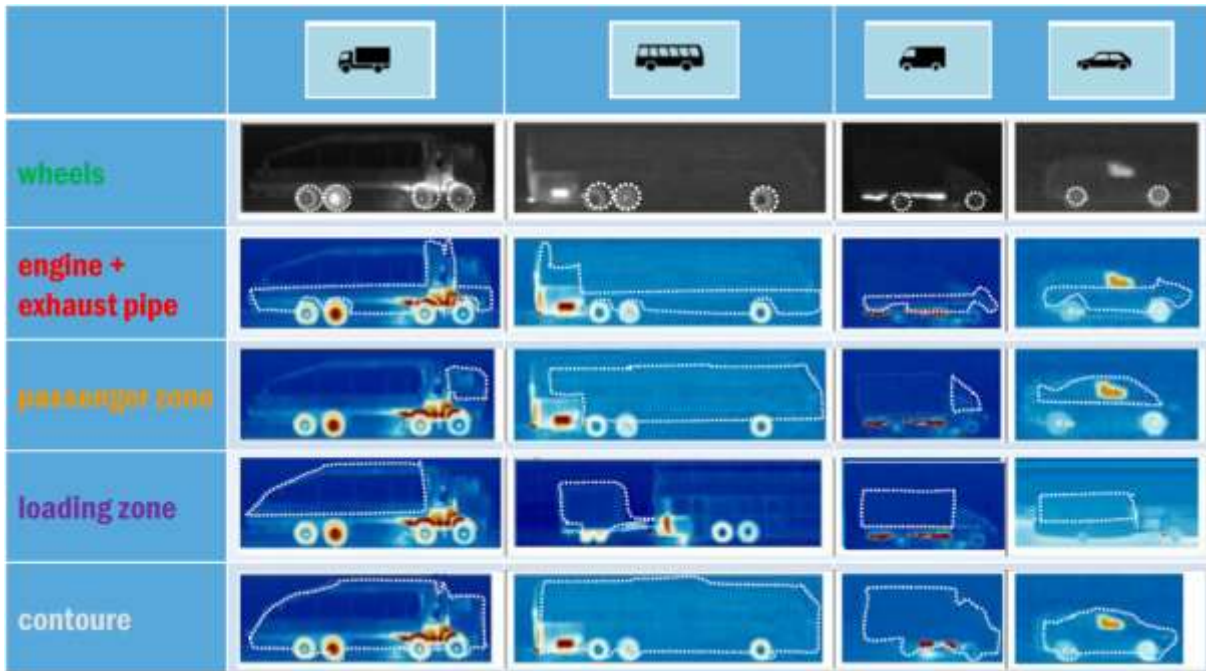


Figure 3 Segmentation of sections of interest by the software in VHD system (SICK)

The original segments and their standard temperature thresholds:

Table 1 Example of temperature thresholds used in road tunnels.

	CarOrVan	Truck	Bus
Contour	460	460	460
Wheel	120	90	70
Load	80	120	80
Passenger	80	80	80
Engine	350	500	350
Reflection	350	500	350
BreakDisc	150	120	120

#### 4.2 Research and development of a LASH FIRE VHD system

To create a LASH FIRE demonstrator the requirements and new functions needed to be implemented and tested. This was developed during the Hazard Identification (HAZID) workshop [5] at the start of the project listed as below.

Table 2 New requirements on the VHD system.


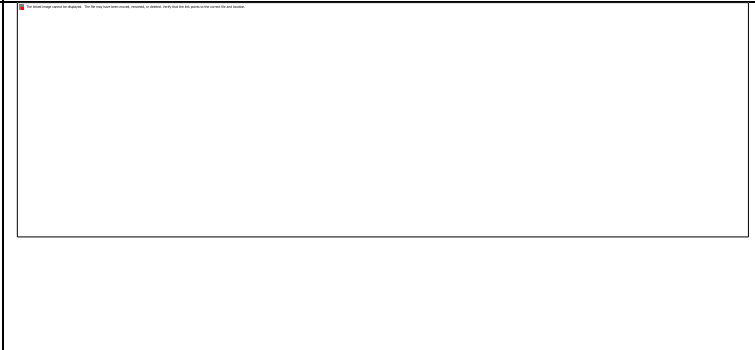
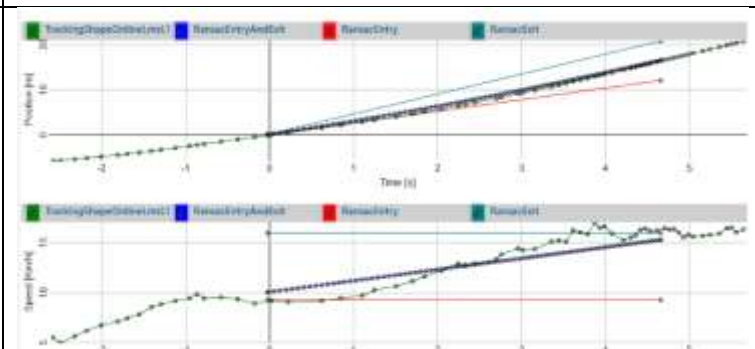
R#	Functional element	Requirement	Test
VL.1	Positioning & profiling, LiDAR	Capture front and rear of vehicle entering the gate using forward LiDAR	VLT 1a
VL1.1	Positioning & profiling, LiDAR	Capture front and rear of vehicle entering the gate using rear LiDAR	VLT 1b
VL.2	Positioning & profiling, LiDAR	Track vehicle as it moves through the gate	VLT2
VL3	Positioning & profiling, LiDAR	Length measurements of vehicle, precision less than 0,4m	VLT3
VL.4	Positioning & profiling, LiDAR	Profiling of the sides of vehicle	VLT4
VL.5	Positioning & profiling, LiDAR	Profiling of the top side of vehicle	VLT5
VT.1	Thermographic profiling, LWIR	LWIR captures the sides of the vehicle	VTT1
VT.2	Thermographic profiling, LWIR	LWIR captures the top side of the vehicle	VTT2

New functions needed to be developed in the TEMS software.


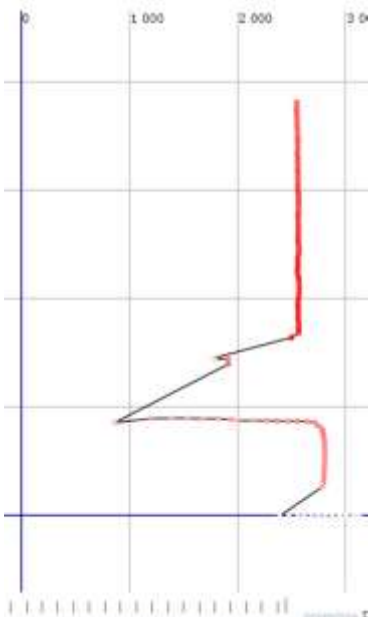

Table 3 New functionality in the VHD system.

F#	Functional element	Requirement	Test
VS.1	TEMS SW development	Incorporate length measurement using two LIDARs	VST.1
VS.2	TEMS SW development	Incorporate downward profiling LIDARs	VST.2
VS.3	TEMS SW development	Incorporate downward thermographic LWIR	VST.3
VS.4	TEMS SW development	Use machine learning algorithm to detect refrigeration unit on trailers	VST.4
VC.1	Clients	Allow presentation of new sensors	VCT.1

During the installation, testing and validation at the demonstration site the development of the desired functionalities in iterations hardware that was installed needed software development and then validation. Below are the results of the process.




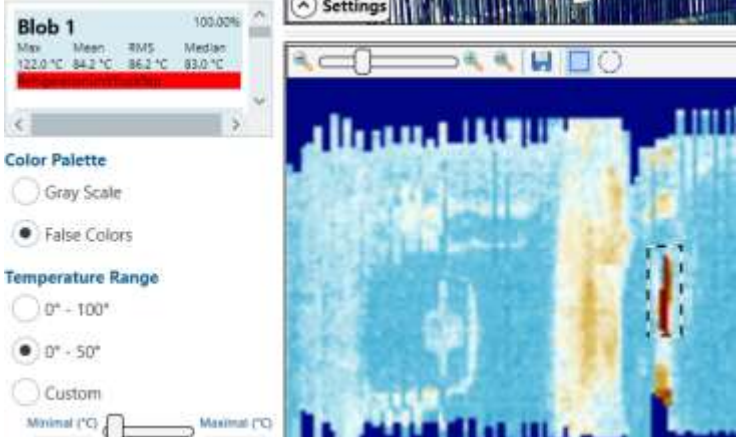
R#	Functional element	Requirement	Test
VL.1	Positioning & profiling, LiDAR	Capture front and rear of vehicle entering the gate using forward LiDAR	VLT 1a
VLT 1a	Front of vehicle entering VHD system. Red circle shows the refrigeration unit on the truck.		
VL1. 1	Positioning & profiling, LiDAR	Capture front and rear of vehicle entering the gate using rear LiDAR	VLT 1b
VLT 1b	Boundary boxes (blue and orange) representing each LiDARs outline of the object, used for positioning and length calculations. Red circle showing the raisable barrier at the gate house.		
VL.2	Positioning & profiling, LiDAR	Track vehicle as it moves through the gate	VLT2
VLT2	Object's speed and position as it passes the VHD system recorded correctly.		
VL3	Positioning & profiling, LiDAR	Length measurements of vehicle, precision less than +/- 0,2m	VLT3
VLT3	Length measurements was better than +/- 0,2m	With the release of TEMS version 3.11 in January 2022 length measurements was better than +/- 0,2m verified by Stena Line.	
VL.4	Positioning & profiling, LiDAR	Profiling of the sides of vehicle	VLT4



<p>VLT4</p>	<p>Right side of truck at the bottom and the refrigeration unit on the trailer at the top as a clear vertical line.</p>		
<p>VLT4</p>	<p>Left side of truck at the bottom and the side of refrigeration unit at the trailer at the top.</p>		
<p>VL.5</p>	<p>Positioning &amp; profiling, LiDAR</p>	<p>Profiling of the top side of vehicle</p>	<p>VLT5</p>
<p>VLT5</p>	<p>Top side of the refrigeration unit on the trailer captured by the right-side CCTV camera as reference to the LiDAR images in VLT4 and 5 below.</p>		



<p>VLT5</p>	<p>Downward facing LiDAR profiling of top side of the refrigeration unit on the trailer. The dip in the line is an opening at the top of the refrigeration AC unit.</p>		
-------------	-------------------------------------------------------------------------------------------------------------------------------------------------------------------------	------------------------------------------------------------------------------------	--

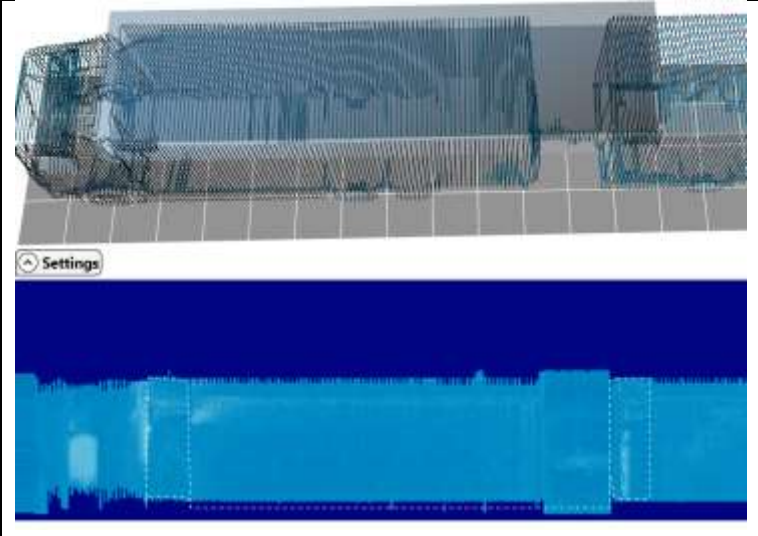
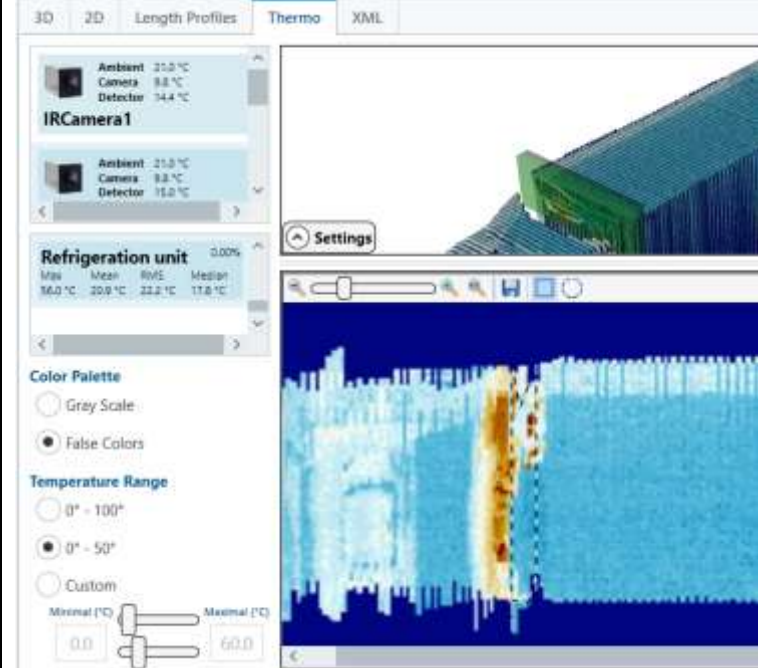

All the requirements for length measurements, positioning and profiling are fulfilled using LiDARs. In parallel the software has been upgraded with the necessary functions and later they have been tuned to increase the performance, and user interfaces upgraded to be able to visualise the new sensors data.

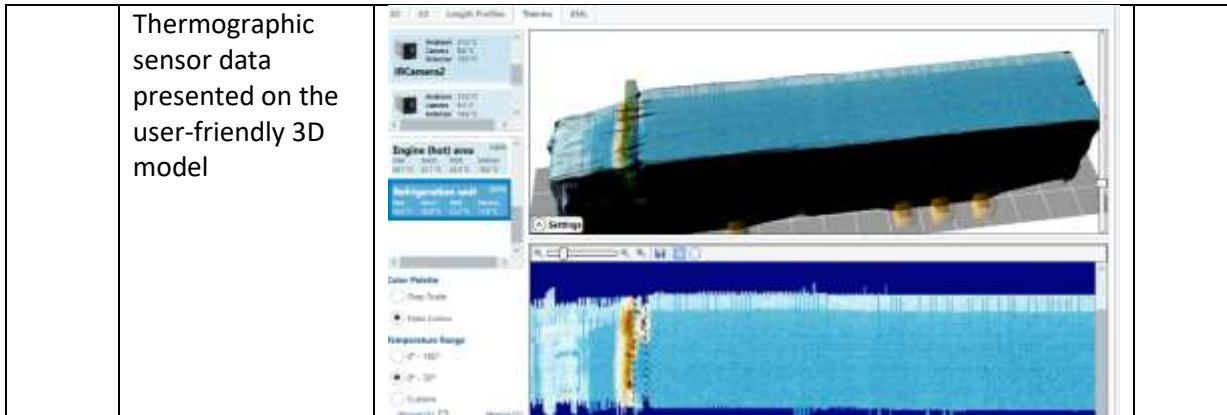
VT.1	Thermographic profiling, LWIR	LWIR captures the sides of the vehicle	VTT.1								
	Right side. Clearly visible behind the truck cabin is the refrigeration unit on the trailer.										
	Left side The sun has heated up parts of the cabin and the top of the trailer. Still the refrigeration unit is visible										
VT.2	Thermographic profiling, LWIR	LWIR captures the top side of the vehicle	VTT.2								
VTT. 2	Top side of vehicle and refrigeration unit with red vertical hot spot, most probably the exposed exhaust pipe from the ICE.										
	User friendly cut out of the refrigeration unit and the triggered alarm.	 <p>The software interface displays a thermographic image of the truck trailer with a red vertical hot spot. A settings panel on the left shows the following data for 'Blob 1':</p> <table border="1"> <thead> <tr> <th>Max</th> <th>Mean</th> <th>RMS</th> <th>Median</th> </tr> </thead> <tbody> <tr> <td>122.0 °C</td> <td>84.2 °C</td> <td>86.2 °C</td> <td>83.0 °C</td> </tr> </tbody> </table> <p>The settings panel also includes options for Color Palette (Gray Scale, False Colors), Temperature Range (0° - 100°, 0° - 50°, Custom), and sliders for Minimal (°C) and Maximal (°C) values.</p>	Max	Mean	RMS	Median	122.0 °C	84.2 °C	86.2 °C	83.0 °C	
Max	Mean	RMS	Median								
122.0 °C	84.2 °C	86.2 °C	83.0 °C								

All the requirements for thermographic profiling of the vehicle are fulfilled.

Table 4 New functionality in the VHD system.

F#	Functional element	Requirement	Test
VS.1	TEMS SW development	Incorporate length measurement using two LIDARs	VST.1
VST.1 t	The boundary boxes illustrate the forward and rear LiDAR used to find the edges (front and rear) of the object		
VS.2	TEMS SW development	Incorporate downward profiling LIDAR	VST.2
VST.2	Downward facing LiDAR presented in the VHD Client as points.		
VS.3	TEMS SW development	Incorporate downward thermographic LWIR	VST.3

<p>VST.3</p>	<p>VHD Client: A truck and trailer, both with refrigeration units. Both refrigeration units are segmented correctly. Big box in the upper is an indication of two refrigeration units that are highlighted as dashed squares in the bottom image.</p>		
<p>VS.4</p>	<p>TEMS SW development</p>	<p>Usage of machine learning algorithm to detect refrigeration unit on trailers.</p>	<p>VST.4</p>
<p>VST.4</p>	<p>The dashed line encircled and indicates the segmentation made by the machine learning based algorithm. The Refrigeration unit's hottest spot is presented, in this case 56°C. A green box is visible as a human friendly visualisation in the upper 3D model.</p>		
<p>VC.1</p>	<p>Clients</p>	<p>Allow presentation of new sensors</p>	<p>VCT.1</p>
<p>VCT.1</p>	<p>3D model using new LiDAR for top-down profiling of refrigeration unit in conjunction with side LiDARs..</p>		



The requirements and the desired functionality in the TEMS, Analyser and Client software are fulfilled.

Using LWIR sensors to create a heat map of each side of the object.

To enable segmentation of the object and user friendliness LiDAR is used to provide accurate measurements of length, width, height and movement of the object. This LiDAR data is fused combining the point cloud with thermographic sensor data from the LWIR to a three-dimensional image of the object.

The segmentation of the object into predefined parts such as wheels and brakes, engine compartment etc. And specially developed for LASHFIRE a possibility to segment out the refrigeration units that can be located on both the truck and trailer was developed.

#### Final choices of software

SICK's developed software platform Traffic Enhanced Monitoring System (TEMS) v. 3.1.1 with the following software modules:

- VHD software module (Hardware interface / Sensor data and image processing / data and alarm output)
- ANPR/DG software module (Hardware interface / data processing and hand over)
- A VHD operator client. Data and alarm visualization for the operator of the VHD system.
- TEMS Analyzer. Extensive data visualization for developers, technicians, and service personnel.

Cameras for reading license plates and ADR/DG placards.

The demonstrator is presented in the delivery D8.9 Prototyping and demonstration of vehicle identification tool, with the sensor array described and software used, and the modification, adding two automatic numerical plate readers. The system uses camera sensors from Micropak, called Micropak 3, both for license plate reading and ADR/DG placard numbers. And for LASH FIRE, developed software for LASH FIRE can now read out license plates on both the truck and trailer as illustrated below.



Figure 4 The principle for ANPR (SICK)

In the LASH FIRE demonstrator, the Traffic Enhanced Monitoring System (TEMS) and the two clients, VHD Analyzer and VHD Client were upgraded with the capability to present the new sensors.

### Back ANPR



Mounted on the south side of the gate house facing north, tilted downwards in approximately 45° that captures the back side of the vehicles.

Figure 5 The ANPR cameras reading the rear of the vehicle. (STL)

**Front ANPR**



*Figure 6 Front ANPR cameras, facing south in the gate house. (STL)*

Below is a side view of the front ANPRs and the rear length and positioning LiDAR with the cut out for better line of sight visible in both the above and below pictures.



*Figure 7 Side view of front ANPRs. (STL)*

**VHD clients**

The user-friendly client software VHD Client for regular users and TEMS Analyzer for super users was used for data collection and demonstration. Below is the VHD Client with a ADR/IMDG vehicle illustrated.





Figure 8 Screen showing a ADR/IMDG marked IBC

In the Operators software client illustrated above, the user receives both audio and visual alarms when they are triggered. The unit is presented in both 2D thermographic and an interactive 3D model. The operator can inspect all three 2D LWIR sensor thermographic images, the temperature range can be changed, above it is set to 0 - 100 Celsius and the colour dark blue is cold and the hot surfaces red. The operator can mark areas and receive spot information all over the object, zoom in/out and in the 3D it is also possible to rotate and zoom in/out.

Important data is displayed on each unit, in this case it is a truck with a cargo of dangerous goods according to ADR/IMDG and the UN 2820 BUTYRIC ACID placard are read and presented. Also, both the truck and the trailers registration plates are presented. An alarm is triggered by the high temperature on the break disk at the middle wheel of the trailer.

Below is a refrigeration unit, visualized in the system administrator client the TEMS Analyzer, the license plate from both the truck and trailer are presented in the vehicle icon column in light blue, the centre pane, and the monochrome images to the right.

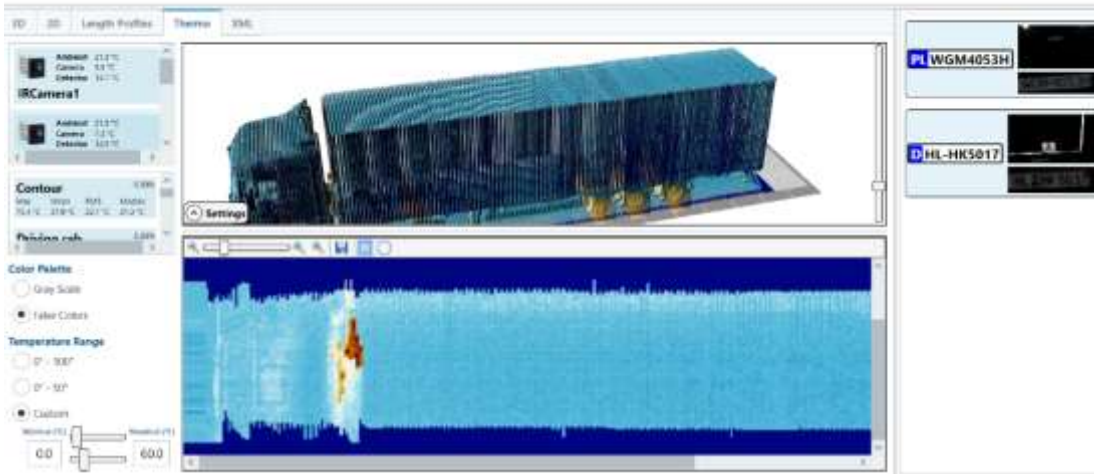


Figure 9 Truck and trailers license plates are read and presented to the operator via TEMS Analyzer user interface.

It has a similar layout as the operator client, but with many more functions for analysing the object and the VHD system.

### ADR/DG placard readers

When the forward ANPR came online in April 2022 the numeric part of ADR/DG placards could be presented in the VHD Client and TEMS Analyzer, later, January 2023 when the rear ANPR also came online, performance increased.



Figure 10 Overheated brakes on trailer with ADR/DG goods.

Above is a cargo of ADR/DG 2820 Butyric acid, the alarm indicated in the VHD Client is the two overheated rear brakes of the trailer.

Below is the rear of the trailer showing a lot of signs and placards viewed through the monochrome ANPR reader.



Figure 11 Rear of the trailer showing signs and placards.

Algorithms scan the picture for known groups and combinations. This is a challenge when other signs and placards are visible to the system. 2820 is then segmented out and presented.



Figure 12 ADR/DG number 2280 placard singled out.

### Visual confirmation

The CCTV placed on the sides can be used as visual confirmation as illustrated below.



Figure 13 ADR/DG placard visible via CCTV.

At the moment the ADR/DG information is handled manually e.g. if the personnel at the terminal is aware that this unit is a ADR/DG they can inspect the unit for the compulsory signs.

#### System of systems

An automatic system could operate alone or be part of an ecosystem contributing to a higher level of situational awareness by sharing information. The LF VHD system could exchange data so it is possible to verify that booked ADR/DG vehicles have or don't have the compulsory placards visible, it could also update the Stowage Planning Tool (SPT) [5] developed in and the LASH FIRE and a future Firefighting Resource Management Centre (FRMC) [6] with what cargo has arrived and if a HVD system was ship borne, what vehicles and cargo is onboard during the loading/offloading operation. Currently there are no such interconnections, and for full functionality on ADR/DG, all sides of the object should be covered by ANPRs.

### 4.3 Finding and segmenting the refrigeration units using machine learning.

The LF VHD systems demonstration is described more in detail in the report D08.10 Demonstration of prototype for detection of potential ignition sources. [4]. And in the first section of 4.2 the developed functionality is described

The sensors installed for thermographic profiling at Majnabbe

The system uses Light Detection and Ranging (LiDAR) and Long Wave InfraRed (LWIR) thermographic sensors.

Two downward facing LiDARs for positioning and length measurement as illustrated in Figure 1 Illustration of the physical installation of a VHD system (SICK) and three for profiling of the vehicle that is processed by TEMS into a 3D model.

LiDARs for positioning and tracking vehicles.

The forward LiDAR mounted underneath the office building prior to the gate house is seen in the picture below.



Figure 14 Forward positioning LiDAR at Majnabbe. (STL)

The rear LiDAR is positioned inside the gate house at the north side shown in the picture below.



*Figure 15 Rear LiDAR for positioning and tracking of vehicle. (STL)*

Also visible is the cut out that was made in the back wall of the gate building. This allows the LiDAR to track the vehicles as they leave the gate house. This increased the precision of the positioning and length measurements so that automatic segmentation was possible.

The LiDARs and LWIR for profiling and 3D model.

On the sides the vertical stack of sensor is mounted as far from the centre line of vehicles path to allow as wide field of view as possible.

**Left side:**



CCTV at the top.

LWIR in the middle.

LiDAR at the bottom.

*Figure 16 LiDAR and LWIR for right side of the vehicle. (RISE)*

**Right side:**

The sensor array for the right side is identical to the left side, the only difference is the ambient temperature sensor visible to the right in the picture below, not visible is the CCTV above the LWIR sensor.



*Figure 17 Sensor array including the ambient temperature sensor. (RISE)*

**Top-down LiDAR and LWIR.**

The LiDAR and LWIR sensors are mounted in line with each other.



*Figure 18 LiDAR and LWIR for left side of the vehicle. (RISE)*



The development and tuning of the VHD system were done in iterations along with SICKs development of TEMS and clients. During Q4 in 2021 there were minor adjustments of sensor positions, and modifications in the software were prepared for the release of TEMS 3.1.1 version in December 2021, with improved precision on tracking, positioning and length measures.

The modifications made for this project show that adding a downward facing LWIR that can capture the heat signature from the refrigeration unit.

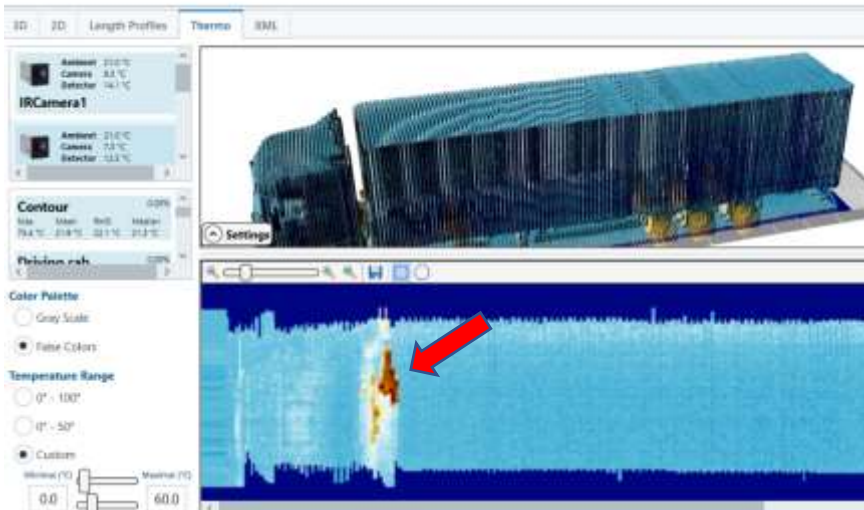


Figure 19 Reefer hotspot highlighted in TEMS SW

The training of the ML algorithms was successful and could be implemented. During the following month the ML picked up refrigeration units on both the trucks and trailers. It gave about 5% false positive selections of objects, but there were no faulty heat signature readings.

Below is an example of a successful segmentation of the refrigeration unit, even if it has very minimal differences in heat signature than the rest of the trailer. The selection is highlighted by the box in the top 3D presentation and the dashed line in the bottom 2D thermographic part.

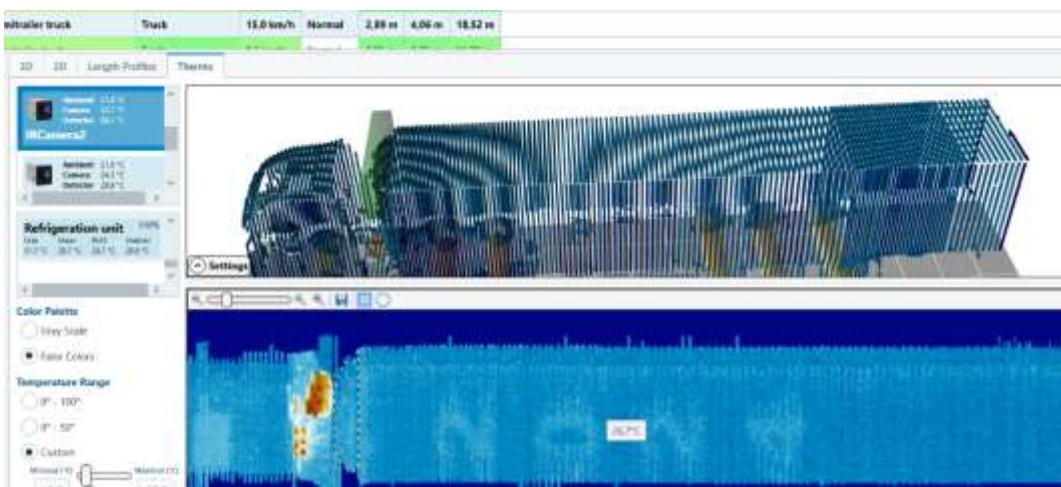


Figure 20 Segmentation of refrigeration unit based on machine learning presented in 2D and 3D.

## 5 Analysis of thermal sensor data collected.

The temperature baseline for the top-down facing LWIR sensor facing the top side of the vehicle’s refrigeration units, showed quite consistent temperature spread during the summer and autumn.

May was the start of the manual collection to the end in October. The data set of 1021 readings of the topside are illustrated below in Figure 21. The dotted black trend line is relatively flat with a small negative trend in the autumn. Lower ambient temperature is probably the cause, and the refrigeration unit has increasingly lower workload as the ambient temperature drops during autumn/winter, and picks up again in the late spring.

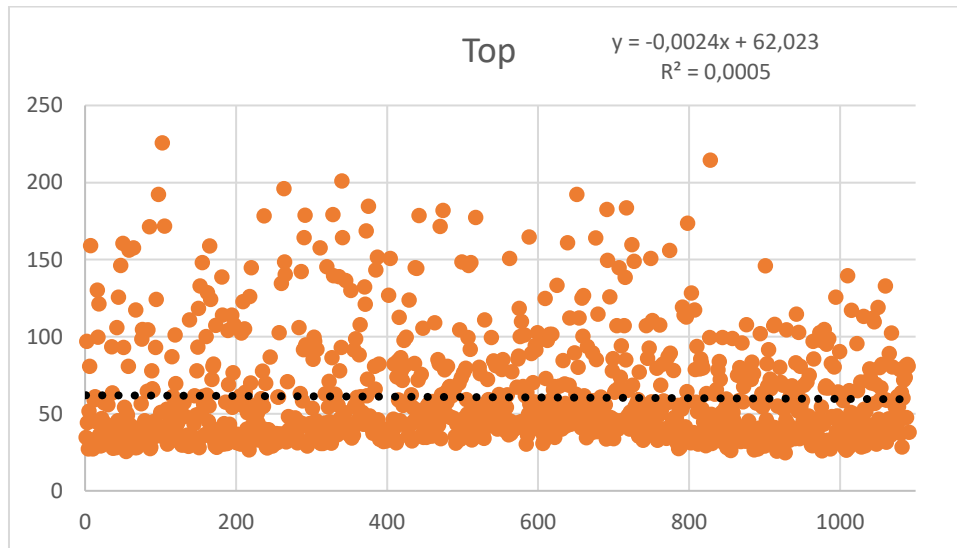


Figure 21 Scatterplot and a trendline of temperature from refrigeration units from the top-down facing LWIR sensor.

The average and median temperatures from the LWIR sensors were calculated from the whole data set of 1021 units.

	Right	Top	Left	AVG
<b>Average (C)</b>	37	<b>61</b>	37	45
<b>Median (C)</b>	36	<b>47</b>	35	40

The correlation value  $R^2$  is calculated to 0,0005 and is extremely low<sup>1</sup>, looking at the plotted readings in Figure 21 above, there is a large temperature range above the linear trend line but narrow below. The right and left side plots can be found in Annex B section. There are many factors that have impact on the temperature spread like:

- Type and manufacturer
- The current workload due the difference between the wanted temperature for the goods and the ambient temperature.
- How recent was the unit started and where is it in its workload cycle: just started or at a rest/idle period.

On top of that, there are many physical aspects to the vehicle, like the age and general condition of the unit, that could add extra variation to a working refrigeration unit.

<sup>1</sup> Right side  $R^2 = 0,0632$ , Left side  $R^2 = 0,0686$

In the following box-and-whisker diagram, the spread on all three LWIR sensors and an average of the three sensors is presented.

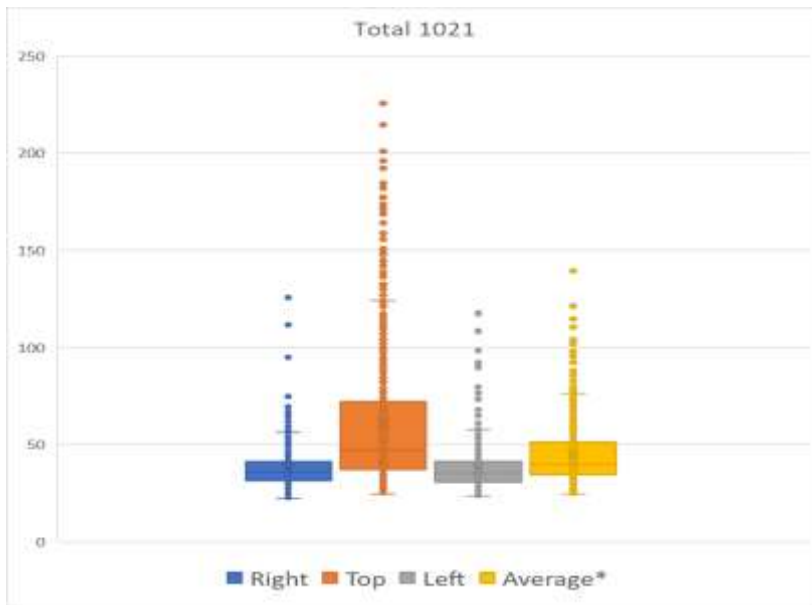


Figure 22 All three LWIR sensors with their spread in degrees Celsius and an average of the three sensors.

The number of outliers from the top-down sensor reading that are above 124 C the top of the fourth quartile, the amount is 68 units. The highest temperature recorded was 226 C. None of these units caused any incidents during their stay at the terminal at Majnabbe or later onboard the ship during the voyage.

The average temperature for the Right and Left side LWIR was ~37 C on the right side and ~37 C left side.

An average of the sides plus the top down LWIR was also calculated as a reference value. This could in a future solution be used to prevent false positives or trigger for outliers by comparing all sides of the refrigeration unit. As shown in the Table 5 below showing the six hottest units captured, the sides of the refrigeration unit do not have to be high when the top shows high temperatures, as shown by number two. The average temperature for the 1021 units is presented inside the parentheses.

Table 5 Temperature of the top six refrigeration units captured in the data set (Celsius).

	Right (37*)	Top (61*)	Left (37*)	Average (45*)
1	58,4	225,7	79,7	121
2	30,1	214,5	39,1	95
3	66,9	201	74,8	110
4	43,0	195,9	73,4	104
5	60,5	192,3	79,7	102
6	125,8	192,3	108,4	139

(\*average)

There is a strong correlation between high temperature readings on the top with warmer than average temperature readings on the sides of the refrigeration unit. Also, the average temperature

for the whole refrigeration unit is higher than the whole data sets average. The hundred highest readings are presented in 13.1 Annex A

For comparison, the temperature used in VHD systems for tunnels on the exhaust pipe is 350 C for cars and busses and 500 C for trucks. The most used temperature thresholds used in VHD systems can be found in 13.3 Annex C

## 6 Usage of machine learning to find refrigeration units.

After training of the SICK developed algorithms, the TEMS system was able to single out truck and trailers with refrigeration units. The ML supported system also successfully picked out units that have a refrigeration unit on both the truck and the trailer as presented below. The refrigeration units are marked out with dashed lines:

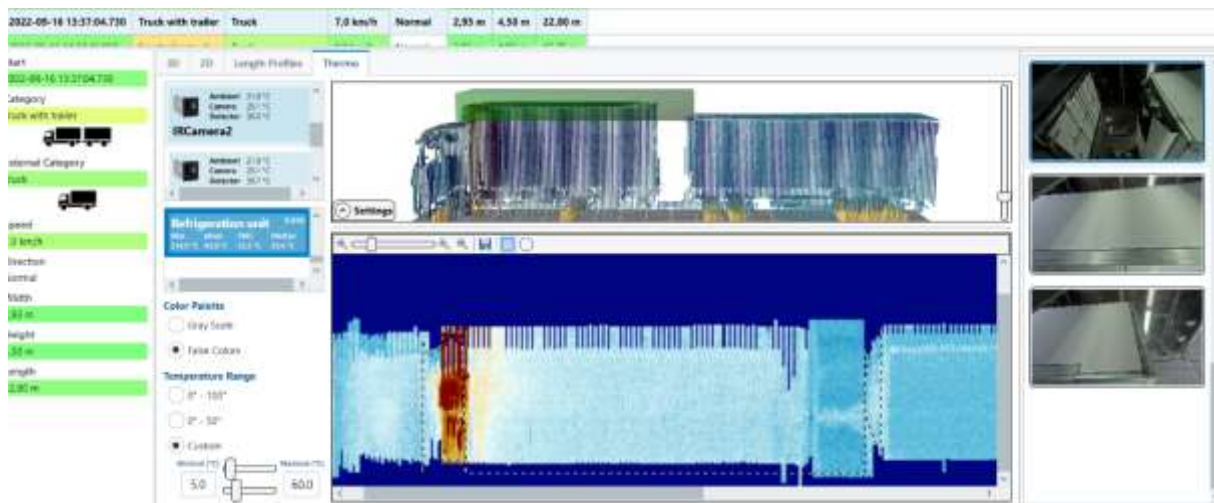


Figure 23 Using ML to find and segment refrigeration units on both the truck and the trailer.

### 6.1 Results from the demonstrator at Majnabbe

From a LF VHD system as in hardware, sensors and software, the developed function for the LASH FIRE project summarized in chapter 4.2, the system can identify refrigeration AC units on both truck and trailers using LiDAR and LWIR. Adding the usage of automatic numerical plate registration and ADR/DG makes it easier to locate a truck or trailer at the terminal. Also, ADR/DG placard readers provides extra critical information. License plate and ADR/DG ties the trailer if unaccompanied to the booking. The VHD system's CCTV cameras provide the users with colour images from all sides of the vehicle and allows the personnel the fastest way to describe the vehicle to all censored parties. The VHD system also provides the lay out of the vehicle with a human friendly visual representation of the vehicle's heat sources, temperature readings and relevant segments of the vehicle in both 2D and 3D. All relevant data is logged, and it is easy for an operator to review the vehicle at any time, as long as the file is stored and accessible.

When a VHD alarm is raised in the VHD System

Reacting on an alarm has been discussed in different forums at Stena Line with personnel from Check-in, stevedores, ship and management.

How to perform an inspection when an elevated risk has been detected, safety of the personnel, driver and passengers are all important topics.

Safety is the uttermost important topic and there are many factors to consider. The crucial aspect is that if an alarm is raised there could be a possible incident imminent. Likewise it could be a too warm component that will cool down to a normal temperature as the vehicle now has reached its destination and will come to a standstill soon, e.g. a break disk or engine component. With a LF VHD system the operator will know much more about the status of the vehicles that enter the terminal or ship information that was unknown before.

In general:

- How to protect the personnel when doing an inspection?
- How to protect other persons in the vicinity?
  
- How to protect other vehicles? Any ADR/DG at the quay?
- How to protect infrastructure at the terminal?
  
- How to safely do the inspection?
  - o Different manufacturers of refrigeration units have different components. Just how to start/stop a unit could be done by an ignition key, flip-switch or push button.
  - o Many refrigeration units do not have an emergency button that stops both ICE and the electrical system.
  - o Handheld Thermal imaging camera?
  - o Ladder access to topside of vehicle?
- How can we train the personnel that will do the inspections?

Then, how to decide if the unit is fit for shipping?

An alarm chain could look as suggested below, where an alarm triggers the shore organization. During the demonstration, three general steps were identified and have been iterated during the demonstration. Depending on where the alarm is received, which could be at the check-in or directly to stevedores or the terminal operator centre, the infrastructure and the response will be different. At Majnabbe the VHD Client was placed at the manned Check-in.



Figure 24 VHD Alarm is triggered.

The VHD operator activates the local support organization at Majnabbe, this is the personnel at the quay that handles the loading operation. Information about the vehicle is communicated, usually over UHF radio and the first goal is to locate the vehicle to start a dialogue with the driver and a first remote assessment of the vehicle. As fast as possible a decision on further actions has to be taken.

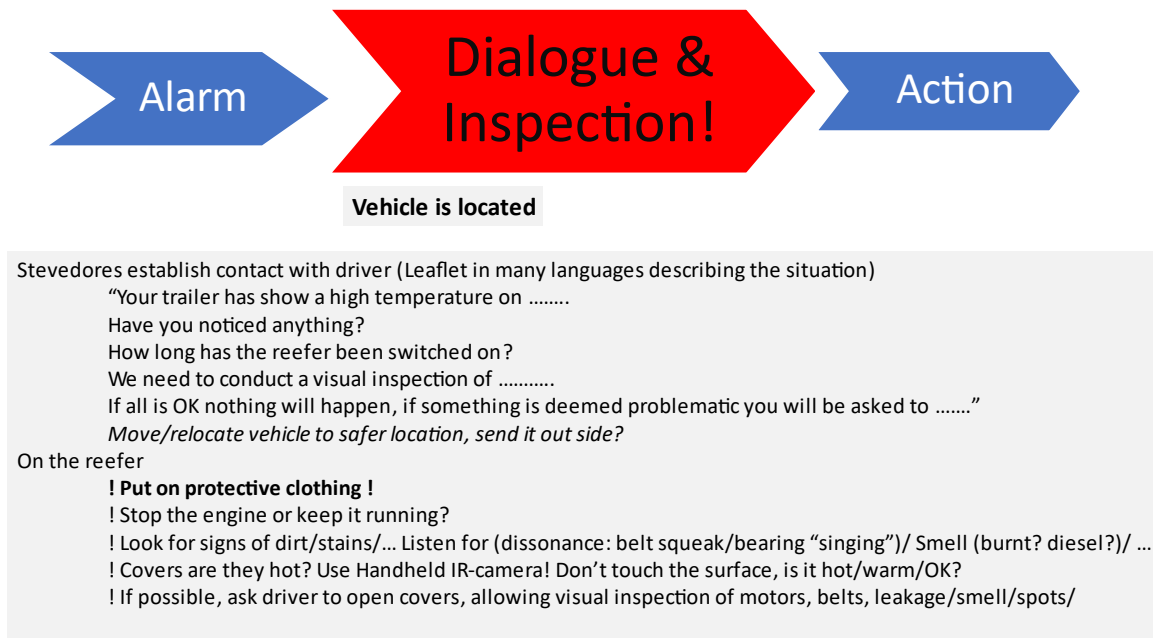


Figure 25 Dialogue with driver and is an Inspection possible to perform?

In the dialogue with the driver, he/she is informed about the situation and information about the vehicle(s) are obtained. The time for action can be short or very long depending on many factors, not only the temperature that has been recorded. Factors like: If it is a ADR/IMDG goods, can it easily be parked at a safer spot inside the terminal for further investigations and service or should it be sent outside directly?



**What do we do now?**

Part of a vehicle is too hot or another malfunction:

**Dialogue with driver:**

“Your trailer has shown a high temperature on ..... The belt is old and needs adjustment or replacement...  
And we ask you to move your vehicle to service spot XYZ we will guide you there.  
You will need to show to us that the equipment is OK before departure”

**Guide driver to correct spot**

- ! Is it possible for the vehicle to get service at the terminal by the driver or service technician?
- ! Is it possible for the driver and vehicle to wait one departure? (is it un-accompanied unit?)
- ! If the driver is unable to correct/service/mitigate problem:

**Contact Check in**

- ? Long time to departure and a overheated wheel break, sufficient time for a cool down?
- ! Close to departure, contact Captain - Can it be strategically placed onboard, could it be loaded on weather deck?

**Masters decision**

Can a suspicious vehicle be separated or segregated from other cargo/vehicles? Extra surveillance/fire patrols?

*Figure 26 What action should be taken?*

Depending on what the situation at the terminal is at the moment, and what the initial discussion with the driver and if an inspection could be performed. Further actions could be required, or the vehicle can proceed and be loaded with extra precaution, such as being stowed on the weather deck. The answer to these and many more questions will vary between companies, terminals, and the captain’s decision regarding the safety onboard his ship.

A VHD system will require new procedures for both the organization at the terminals as well as onboard the ship. These procedures will update the companies’ Safety Management Code.

## 7 Automated Guided Vehicle

Main author of the chapter: Leon Sütfeld, RISE



Figure 27 Render of the final version of the AGV

The compact AGV prototype designed to be able to run underneath the majority of vehicles illustrated in Figure 27 used tracks for good traction on uneven surfaces and precise manoeuvring.

### 7.1 Final choices of hardware

This section covers information on the hardware used in the AGV and the motivations for why it was chosen. A general note on the hardware is that for the harsh environment in the ship, waterproofing will be necessary, but has not been applied for the demonstrator.

#### 7.1.1 Chassis

The lid of the AGV is attached with screw posts and screws. Spacers are employed to ensure a level surface, which is required for the LiDAR (section 5.1.3) to function properly. The interior components of the drone are mounted using double sided tape, brackets, or bolted connections through the AGV's floor. These differing means were used depending on the properties of the components that needed to be fixed: batteries for instance, are mounted with double sided tape to not over-constrain them as they can swell slightly while charging.

The electrical connections inside of the AGV are realized with silicone wire, which has a high degree of flexibility when it comes to arranging the components. To allow for rapid changes when needed, WAGO connectors were used when applicable.

#### 7.1.2 Batteries

The batteries used are regular consumer LiPo batteries, which are commonly used for remote controlled vehicles. To match the voltage needed for the onboard Jetson processing unit and the RoboClaw motor controller, 4S (4 cell) batteries were chosen resulting in a nominal voltage of 14.8v which was within the accepted input range of the onboard devices.

Using consumer OTC batteries made them cheap to acquire, but had some drawbacks, which are discussed in further detail in section 9.3.

#### 7.1.3 LiDAR

A LiDAR sensor is used to provide the necessary information for e.g., mapping of the AGV's environment, navigation and collision avoidance. If used solely for navigation purposes it could be possible to have a limited angle, given that it could provide enough information for a SLAM system to



recognize its current position. SLAM stands for Simultaneous Localization and Mapping, which is a method of creating maps and finding one's relative coordinates by means of triangulation based on detected landmark points from sensors. For a collision avoidance system, however, a limited angle would likely not be enough as it may have to avoid not only objects in front but from all angles and in the case of an aerial drone above and below as well.

The LiDAR used for the AGV is the YDLIDAR G4 [8], which has a height of 4 cm and a detection range of 16 m. Given that the drone will operate indoors in environments sufficiently filled with static objects, a range of 10-15 m was deemed sufficient. Further testing is still needed as the navigation might not be able to gain sufficient information in those ranges when object density is sparse, as would be the case in a (partially) void cargo deck on a ferry. The rotation rate of the YDLIDAR G4 is up to 12 Hz. Given that the sampling rate is high enough the maximum delay with which an object should be detected is about the rotation rate. There is also a delay in processing and sending the required data, which will be added to the total reaction time of the systems.

#### 7.1.4 Camera RGB

A type of simple sensor to use for object detection is the RGB camera. It is a common sensor for the purpose, it can also be both cheap and easily accessible. One of the challenges to take into account is the light conditions inside of the ship's hull and furthermore underneath vehicles. The license plates in question are generally located between the vehicles, which provides some shadowing other than the general light conditions in the ship's hull, but not to the extent of the undercarriage of the vehicles and cargo. Other requirements that needed to be taken into consideration were the compatibility with the rest of the system operating on a Linux based processing platform, and with USB connectors, as the readily available alternative for communication between the camera and the processing unit.

With these conditions in mind, the Logitech Webcam C930e [9] was chosen, since it is a RGB camera, compatible with Linux, 90-degree field of view, and it enables 1080p HD streaming at 30 frames per second. It is functional as a standard RGB camera, but for a more developed AGV concept it could be beneficial to consider a smaller camera that can be mounted in the case of the AGV.

#### 7.1.5 Processing unit

For the AGV to function and process all the incoming data from the sensors a processing unit is necessary. To allow for a quick response time a mobile processing unit that could be placed in the AGV was chosen. Among the potential candidates, the Nvidia Jetson [10] product line was the most appropriate option. The model choice fell on the NVIDIA Jetson AGX Xavier dev kit. At the time of constructing the drone this was the most powerful choice in terms of processing power, while remaining small enough to fit inside of the AGV and stay underneath the scan field of the LiDAR. Additionally, it has strong GPU processing power, which ended up not being utilized with the current construction of the drone. However, it could be beneficial if e.g., more machine learning oriented approaches would be used in the future.

#### 7.1.6 Thermal Camera

The AGV is fitted with Long Wave Infrared (LWIR) micro thermal camera module from FLIR, model Lepton 3.5 [11]. This also has the potential to be mounted on a PureThermal-2 FLIR Lepton smart I/O module from GroupGets [12]. The final dimensions of this setup are 30 x 22 x 8 mm. Some of its most interesting specifications are listed below:

- Optimum Operating Temperature Range: -10° to + 80°C
- Thermal sensitivity: < 50 mK

- Spectral Range: 8 - 14  $\mu\text{m}$ , i.e., LWIR
- Resolution: 160 x 120 pixels
- Pixel Size: 12  $\mu\text{m}$
- Frame Rate: 8.7 Hz
- Radiometric accuracy
  - High gain:  $\pm 5^\circ\text{C}$  @ 25 $^\circ\text{C}$
  - Low gain:  $\pm 10^\circ\text{C}$  @ 25 $^\circ\text{C}$
- Scene Dynamic Range
  - High Gain Mode:  $-10^\circ$  to  $+140^\circ\text{C}$  @ 25 $^\circ\text{C}$
  - Low Gain Mode:  $-10^\circ$  to  $+400^\circ\text{C}$  @ 25 $^\circ\text{C}$
- Horizontal Field of View (HFOV): 57 $^\circ$
- Diagonal Field of View (DFOV): 71 $^\circ$
- Lens Type: f/1.1
- Power Consumption: 150 mW typical, 650 mW during shutter event, 5mW standby

For the thermal camera to achieve the purpose of scanning the underside of vehicles or cargo for irregular heat signatures it is paramount that it achieves a sufficient coverage, i.e., the parts of interest in the cargo need to be within the thermal camera's frame at a distance where it is able to read the values with precision. One of the primary factors to determine the footprint is the height of vehicle or cargo from the ground as it will increase the distance between the drone and the underside. The ground clearance or ride height of vehicles varies depending on the type. Between different vehicles the ground clearance can significantly differ. To give a few examples, a Porsche 911 GT3RS has a height from the ground of 88mm, compared to 14 cm of a Tesla model 3. The Rivian R1T or a R1S are significantly higher at 37.8 cm. This variation can make it challenging to find a setup for the thermal camera that achieves the best coverage. In extreme cases the drone may not even be able to enter underneath a vehicle. This has been a major point of interest during the design as keeping the height of the drone low affects its ability to both scan underneath the vehicles and to move underneath them at all. There are, however, limits to how low it can be designed while still containing all the necessary components to operate. For the calculations and visualizations in this report an assumption of vehicle ground clearance has been set at 15 cm, as it is a realistic value for most current EVs, and the drone cannot reasonably be expected to function far below this ground clearance unless significant changes are made to its design.

In Figure 28 three illustrations can be found; Top: AGV approaches vehicle with a battery of 1.60m width and 15cm ground clearance. The red cone depicts the field of view (FOV) of the IR camera and how it intersects with the battery. Middle: The thermal sensor is mounted with a fixed angle of 20 $^\circ$  on the AGV. It has a horizontal FOV of 57.1 $^\circ$ , and a vertical FOV of 43.48 $^\circ$ . Bottom: The intersection of the FOV cone with the battery shown in light grey. The full width of the battery is visible in the IR camera's frame at 157.2cm distance.

A part of the benefits with the 3D model of the drone described is the ability to approximate the thermal camera's footprint while moving under a vehicle. While it is not a perfect representation of reality it creates an environment where it is easier to make modifications while examining their effects on the system. This setup makes it possible to visualize the footprint and estimate how well the coverage will be for different vehicle heights, in addition to choosing an appropriate angle for the thermal camera. As can be seen from Figure 28 one camera is able to fully cover the undercarriage at a distance of roughly 1.5 m, which close enough to achieve acceptable resolution. An angle of 20

degrees from the vertical plane, as seen in Figure 11, was deemed appropriate for the thermal camera based on a visual inspection of the alternatives in the 3D model.

From the experiment visualized in Figure 28 the camera footprint is shown. Note, the camera footprint is not the FOV, as FOV is the size of the image on a flat plane perpendicular to the lens at a given distance. Also, due to the tilted image plane (i.e., not being perpendicular to the optical axis) and a  $f_{\#} = 1.1$  (according to specs. of the thermal sensor) out-of-focus artifacts will be present. However, Scheimpflug adjustments are beyond the scope of the current prototype.

The 3D modelling results showed that the usage of one FLIR Lepton thermal camera was a promising choice if it was placed at a correct angle. The height of the vehicle or cargo does still present a major factor of how large the coverage of the camera is. However, even at relatively low ground clearances, such as 15 cm, the drone can be able to cover the whole width of the vehicle at a distance of approximately 1.5 m. This measurement does not take into consideration cases when the undercarriage is not perfectly flat, but it provides a good indication that the sensor will be sufficient for the task.



Figure 28 Coverage of a typical passenger vehicle's battery with the IR camera.

## 7.2 AGV 3D model

A 3D model of the AGV was created in Blender [13] to facilitate component selection and hardware layout choices. It also enabled the design of 3D printed hardware parts and served as a reference for the AGV's dimensions and as a visualization tool.

The 3D model allowed us to test various component layouts with a multitude of potential components quickly and efficiently before ordering any of them. This saved us large amounts of time and money and enabled tight packaging of components in the chassis.



*Figure 29 Render of the AGV's final internal component layout.*

The above image is a render of the AGV's final internal component layout, including the Nvidia Jetson AGX Xavier (bottom left), RoboClaw motor controller board (red) motors (top left and bottom right), batteries (center right), USB extension card (top right) and remote receiver (top left, black).

It further enabled precise planning, for instance of the camera angles, and led to the creation of three 3D printed custom hardware pieces; a protective guard for the rear toggle switch, a bracket to keep the RGB camera in a fixed position, and a mounting bracket for the IR camera. The latter was designed to keep the IR camera at a 20° upward angle, which was deemed ideal based on a 3D simulation of the camera's field of view (see Figure 30).



Figure 30 Renders of the custom hardware pieces on the AGV.

The rendering in Figure 30 illustrates the custom hardware pieces on the AGV. Top and middle: RGB camera bracket (wedge-shaped support for the arm holding the camera's body) and IR camera mounting bracket. Bottom: Protective guard for the toggle switch.



Figure 31 Render of an earlier version of the AGV with a visual depiction of the IR camera's field of view.

The rendering in Figure 31 of an earlier version of the AGV with a visual depiction of the IR camera's field of view (red) at a 20° upwards angle and intersection with the floor of a typical passenger vehicle (dark grey).

### 7.3 Final choices of software

Automatic navigation and locomotion of the AGV is realized by a sense-plan-act control architecture, as depicted below. Additionally, license plate detection and thermal image analysis is embedded in the main control program and run in parallel with the navigation and locomotion tasks.

Due to compute constraints, different modules (blue boxes in the figure below) of the navigation and locomotion architecture are running in parallel processes on the main compute device (Nvidia Jetson) at different update rates. While most of the navigation-related modules (left half in the figure) run at a maximum frequency of 5 Hz (mutable parameter), the PID controllers for precise motor control require higher update rates and run in a parallel process at 50 Hz (mutable parameter). The license plate detection and temperature readout modules (top right in Figure 32) each run in additional parallel processes on the same device.

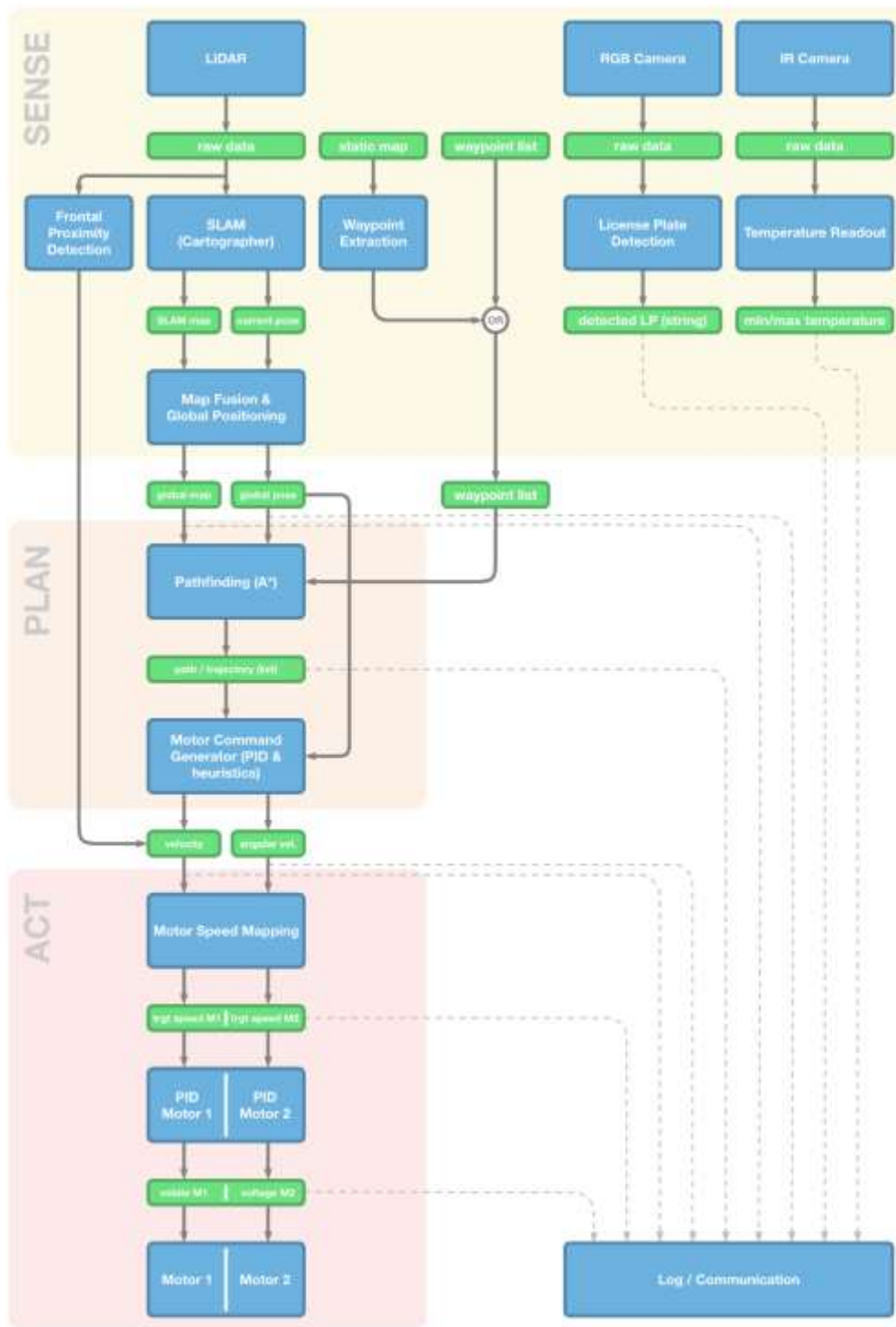


Figure 32 Conceptual sketch of processing flow (sense-plan-act control architecture, license plate detection and thermal imaging)

### Mapping

The basis for the AGV’s automated navigation and locomotion system are 2D maps of the environment around it. They provide knowledge of obstacles and the AGV’s absolute position within its environment for the subsequent path planning algorithm.



Simultaneous Localization and Mapping (SLAM) is performed based on the raw data provided by the YDLIDAR system, using the Cartographer software package. The Cartographer project [14] offers a code base that performs SLAM based on either 2D or 3D LiDAR data. It is mainly based on C++ and the code is provided under an Apache-2.0 license. The core program has been ported into several systems, such as ROS, Turtlebot and Fetch. Based on our testing, the system's capabilities are in line with the requirements for the navigation software, returning accurate maps of the AGV's environment and tracking the AGV's position within that map accurately, provided there are enough detectable features in the environment.

The output of the SLAM system is (1) a grayscale map in which pixel values represent the cumulative evidence over time for obstacles in any given location, and (2) the AGV's current position and starting position (origin) within this map. The scaling of this map is fixed at ca. 1.1cm per pixel. As the AGV moves within the environment, the outlines of obstacles (e.g., the vehicles' wheels) in the SLAM map become more and more clear, while empty space becomes solid black over time. We apply a threshold to this map, as the path planning algorithm requires a binary map as input.

The map provided by the SLAM system is then corrected for rotational and translational offsets and merged with a manually constructed static map of the environment (e.g., the ship's cargo deck) into a (joint) global map. The static environment map is scaled to match the SLAM map at 1.1cm per pixel and contains the outer perimeter of the area to scan, as well as static obstacles and information on the location and orientation of a calibration rig. The calibration rig is essential for the determination of translational and rotational offsets between the two maps and is described in more detail in section 5.8.2. To save on computational resources, the global map, i.e., the superimposition of the static environment map and the dynamic SLAM map is scaled down by a factor of 1:5, resulting in a scaling of ca. 5.5cm per pixel (the scaling factor is a mutable parameter).

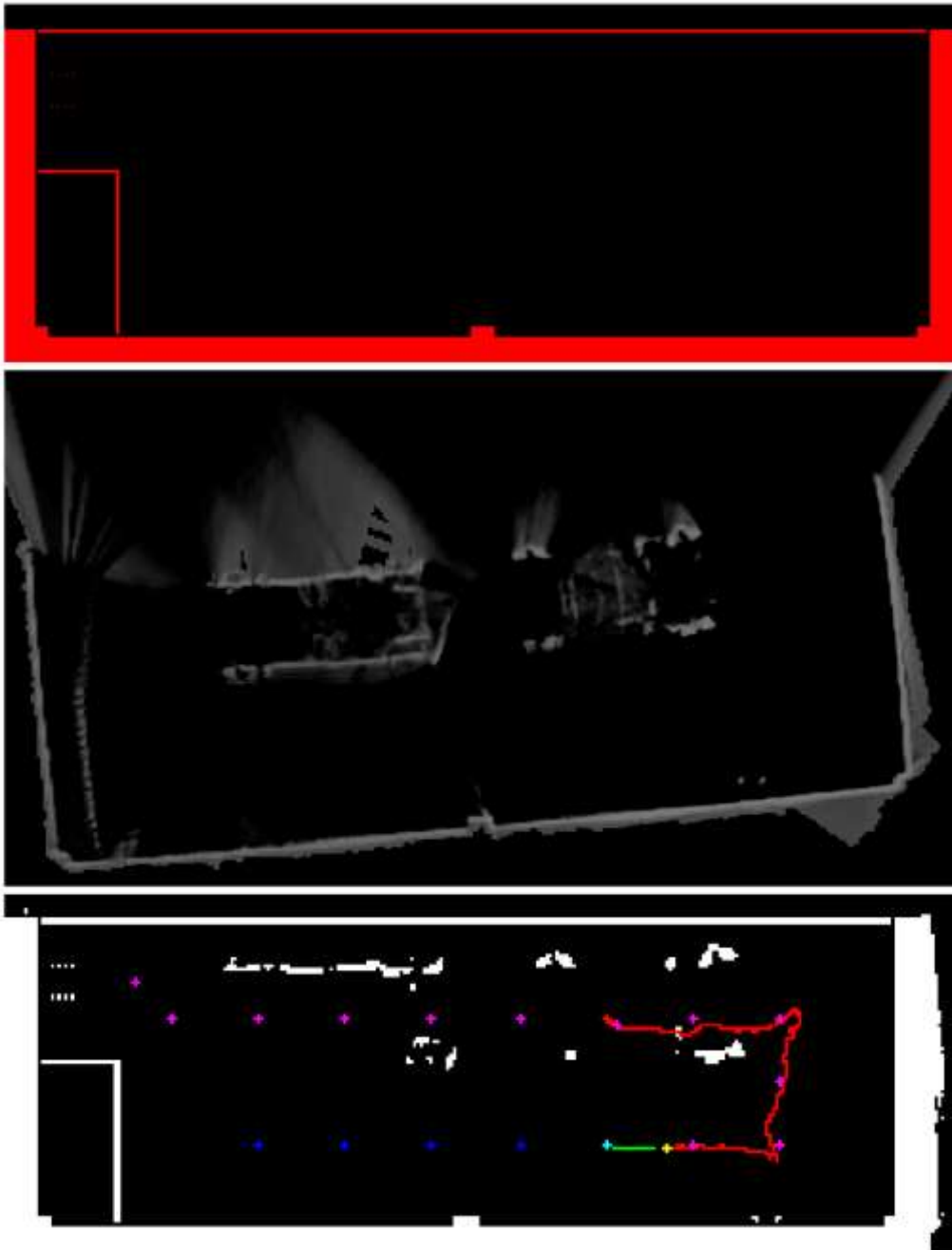


Figure 33 Top: static environment map, middle: dynamic SLAM map (unprocessed), bottom: global map.

In the image above at the top: static environment map, middle: dynamic SLAM map (unprocessed), bottom: global map, i.e., downscaled superimposition of static environment map and SLAM map after alignment and thresholding. Solid objects indicated in white, completed waypoints in pink, current waypoint in turquoise, future waypoints in dark blue, current position of the AGV in yellow, most recent trajectory in red, path to the next waypoint as determined by the A\* algorithm in green.

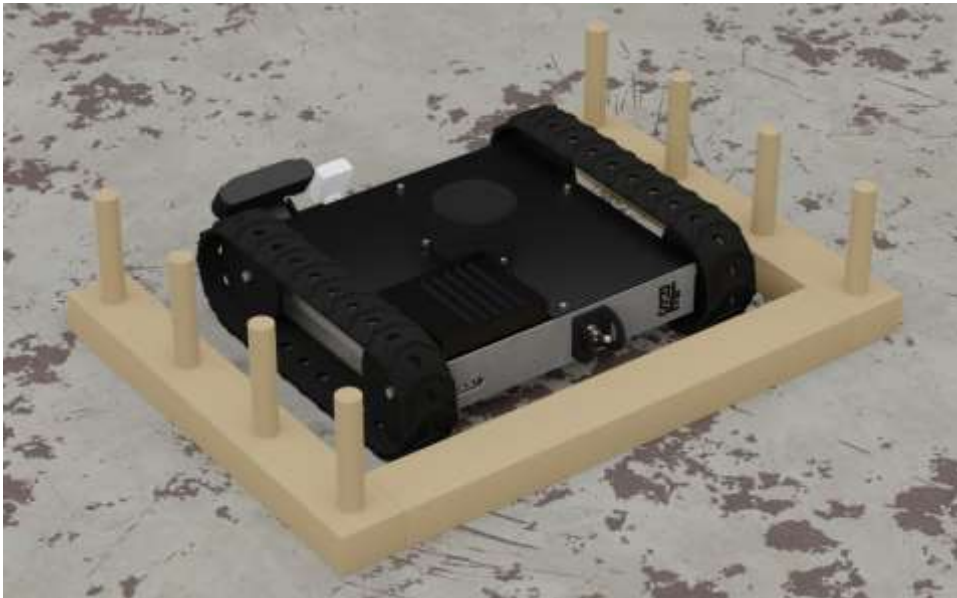
#### Calibration

The calibration procedure serves to determine accurate translational and rotational offsets between the static environment map, the SLAM map, and the AGV's tracked pose within it. It is essential for the accurate mapping of the dynamic SLAM map and the AGV's current pose at any given point in time into the coordinate system of the static environment map.

A calibration rig was specifically designed and built for this use case as part of this work package. It measures 41.9cm long by 57.6cm wide and features two rows of four vertical columns each that slightly surpass the AGV's height at 14.3 cm height. At the beginning of each scan run, the AGV needs to be placed within the calibration rig, where the eight columns create an unmistakable fingerprint in the LiDAR's output.

The calibration procedure identifies the four corner columns and uses their locations to triangulate the AGV's pose relative to the calibration rig, i.e., it computes the translational and rotational offset of the AGV from the precise center location and "true north" orientation of the rig. The calibration rig itself is to be mounted in a fixed position inside of the environment, the position and orientation within the environment are measured and provided as input parameters to the map merging algorithm.

With this, the pose of the calibration rig on the static environment map, the SLAM maps origin relative to the calibration rig, and the AGV's pose relative to the calibration rig are known, allowing for a precise translation between the different coordinate systems. As the SLAM system provides the AGV's pose relative to the SLAM map's origin, this too can be continuously translated into the global map's coordinate system.



*Figure 34 Render of the AGV placed in the calibration rig.*

### Navigation and path planning

In dynamically changing environments, a fixed path for the AGV would prove problematic, as no complete path covering a larger environment can be guaranteed to be permanently free of obstacles. Since vehicles and potentially other cargo are unlikely to be placed in the exact same place for every journey or on every ship, it is preferable to use an adaptive algorithm that can find an effective path given the current situation.

To this end, we provide target waypoints for the AGV to reach, and since the direct (straight line) path between target points may be blocked by obstacles, we employ a dynamic path finding algorithm to find a free path from the AGV's current position to the next waypoint.

The manually defined waypoints are provided to the system either as a list of (x, y) coordinates relative to the origin of the static / global map, or via markers (green pixels) drawn directly into the map and can be placed arbitrarily far apart. The dynamic path finding is done via the A\* algorithm.

The implementation of A\* on the AGV is based on open-source python code [15] but was largely rewritten for computational efficiency and robustness. The path finding algorithm takes into account any obstacles (white pixels) present in the global map and leaves a margin slightly larger than the radius of the drone around them. A waypoint is considered reached as soon as the AGV's center is within 30cm of it (mutable parameter), at which point the next waypoint will be selected as target.

If a waypoint lies within or too close to a detected obstacle or all paths to it are blocked off by obstacles, the waypoint is reset to the nearest location that is deemed reachable by the AGV.

#### Path following / locomotion

Path following describes the processes involved in going from locations on a map (i.e., the pose of the drone and the path ahead) to direct motor commands and the actual locomotion of the AGV.

The implementation of path following on the AGV is comprised of three steps: First, target values for forward velocity and angular velocity (i.e., steering) are computed based on the path ahead provided by the path planning algorithm. Second, the target values for forward and angular velocity are translated into target speeds for the two motors. Third, the target speeds for the motors are translated into voltage outputs and sent as commands to the motor controller board, and by extension the motors themselves.

Computing the target *forward* velocity is done by a heuristic that considers (1) the angular offset between the AGV's current heading and a line towards the next point on the path, and (2) the overall amount of rotation required to follow the subsequent steps of the path. In simpler terms, the straighter the path ahead looks from the AGV's point of view, the higher the targeted forward velocity.

The accompanying targeted *angular* velocity then is computed by a PID controller, in which the offset between the AGV's current heading and a line towards the next point on the path is used as the error term. By modifying a signal (in this case angular velocity), PID controllers regulate a measured outcome variable (in this case the offset between AGV heading and path ahead) to reach a target outcome (in this case 0).

The target values for forward and angular velocity are next translated into target motor speeds. The forward velocity of the AGV in meters per second is proportional to the speed of the two motors (in arbitrary units, as provided by the motor encoder readout). This translation factor was measured and is applied as a parameter in the translation. For tracks-based vehicles, steering is not performed by turning wheels around the z-axis, but instead by differential speeds of the left and right track, or the motors driving them, respectively. Thus, the targeted angular velocity is translated into motor speed differentials that are then added to the targeted forward motor speed, resulting in individual target speeds for the left and right motors (M2 and M1 respectively).

Finally, the commands sent to the motors are a direct representation of the voltage levels controlling their rotation, provided as 8-bit signed integer values that cover the range from maximum negative voltage to maximum positive voltage with values between  $-127$  and  $127$ . However, there is no one-to-one correspondence between voltage levels and motor speeds. The mechanical resistance the system has to overcome can and does vary due to both internal and external factors, such as uneven internal motor resistance over the course of a revolution, or varying resistance / grip levels of the underlying surface. To achieve good control over the motors' output speed, we employ two further PID controllers (one for each motor) tasked with controlling the motor commands to reach and maintain the individual motors' target speeds. Doing this requires a fast control loop, which led us to run the motor control PIDs in a parallel process to the primary navigation loop, running at 50Hz.

This step completes the navigation and locomotion signal flow in its basic form.

### Collision avoidance

Collision avoidance is implemented in basic form by the pathfinding algorithm described above, as paths are planned around the obstacles detected in the map. However, while the SLAM system is well suited to detect stationary obstacles, objects typically need to be stationary for several seconds until enough evidence has accumulated to show a clear outline on the map. Dynamically appearing obstacles, such as people walking in front of the AGV or falling objects, are not reliably detected.

To avoid collisions with dynamically appearing obstacles, we additionally implemented a frontal proximity detection algorithm that analyses the raw data stream coming from the LiDAR. Concretely, it detects any objects that are positioned within a rectangular area in front of the AGV. This area has the same width as the AGV and extends 10cm out from the front of the AGV (mutable parameter).

When an obstacle is detected within this defined area, the forward velocity signal is immediately set to 0, while angular velocity remains unchanged. This way, the AGV remains stationary until the obstacle has either disappeared or is detected by the SLAM system, which then allows for a route to be planned around the obstacle. As the angular velocity term remains unchanged, the AGV can turn on the spot and resume operation once a path around the obstacle has been found.

### License plate detection

In order to identify objects that are more likely to become ignition sources, primarily EVs, an approach to detect license plates has been chosen. A license plate number of a transport can provide significant information, such as age and vehicle type, if combined with a license plate database or a loading log for the ship where this information has been added. The chosen version of license plate readers is OpenALPR [16], open-source Automatic License Plate Recognition. It is licensed under GNU Affero General Public License v3.0 and written in C++. There are, however, bindings to Python, which is the main programming language used in this project. The program finds license plates in images and outputs a list of the most likely candidates of plate numbers ranked by confidence.

### Hot spot detection

The software needed for the Lepton 3.5 IR camera in this setup is developed by GroupGets. The shared library of “libuvc” [17] was copied to the working directory of the AGV NVIDIA Jetson, and the python code “uvc-radiometry.py” (provided in “purethermal1-uvc-capture” [18]) was modified to allow for the extraction of sensor data (temperature readouts) from the IR camera.

## 8 AGV test and demonstration

### 8.1 Functional requirements and tests

#### Test design

The control architecture of the automated driving functions (see Figure 32 above) and the predominantly serial nature of the signal flow within it create a chain of dependencies between earlier and later modules. Later modules typically require all earlier modules to be functional and/or their output to be sufficiently accurate. In many cases, test documentation for modules later in the chain simultaneously document the functioning of earlier modules.

We created a list of isolated functional requirements for all major functional elements of the architecture and document the meeting of these requirements in either specific isolated tests or in combined / full system tests.

## Scenario description

In the following, we list the functional requirements for the AGV and the corresponding test scenarios to verify that the requirements are met.

### Functional requirements:

Table 6 AGV Functional requirements.

R#	Functional element	Requirement	Test
8.1	localization & mapping	static environment map is loaded correctly	T3.1
8.2	localization & mapping	dynamic environment map (via SLAM) is created and sufficiently accurate	T3.1
8.3	localization & mapping	scaling of static map and dynamic map match with sufficient accuracy	T3.1
8.4	localization & mapping	offset-correction between static map and dynamic map is sufficiently accurate	T3.1
8.5	localization & mapping	static and dynamic maps are merged correctly into global map	T3.1
8.6	localization & mapping	AGV location tracking on global map is sufficiently accurate	T3.1
9.1	motor commands	individual motor control via python control command functional	T1.1
9.2	motor commands	motors reach and hold constant a requested motor speed	T1.1
9.3	motor commands	AGV movements reflect requested forward velocity and angular velocity with sufficient accuracy	T2.2/ T3.1
10.1	navigation	waypoint list is correctly read from text file	T3.1
10.2	navigation	waypoint list is correctly created from markers on static map	T2.2
10.3	navigation	pathfinding algorithm finds path from current position to target waypoint	T2.2/ T3.1
10.4	navigation	planned path is followed by appropriate forward and angular velocity commands	T2.2/ T3.1
10.5	navigation	collision avoidance: AGV stops when encountering dynamic obstacle in front of it	T2.1/ T2.2
10.6	vehicle identification	vehicle identification via license plate recognition in lab environment	T2.3
11.1	system	vehicle navigation functional in relevant real-world scenario (isolated)	T3.1
11.2	system	temperature and license plate readout functional in relevant real-world scenario (isolated)	T3.2
11.3	system	vehicle navigation, temperature and license plate readout functional in relevant real-world scenario (combined)	T3.3
13.1	battery	battery life sufficient for targeted scenario	T4.1

## Test scenarios:

Table 7 AGV Test scenarios.

T#	Test Scenario	Description
1.1	PID motor control isolated	Target motor speeds are defined and scheduled, and sent to the PID controllers, which create command signals to the motors. The motor speeds are then read out and compared to the requested speeds over time.
2.1	Collision avoidance for dynamic obstacles (lab test)	The AGV is tasked with reaching a waypoint on the map. While it moves towards the target, an obstacle is held in its path, and the AGV is expected to stop before a collision with the obstacle occurs.
2.2	Navigation in lab environment	A parcours with a series of waypoints is defined in a lab or office environment. The AGV is tasked with visiting all reachable defined waypoints while avoiding any obstacle collisions.
2.3	Vehicle identification in lab environment	Testing the license plate detection software on a static dataset of European license plates.
3.1	Navigation in relevant environment	A parking garage with parked vehicles is used as an approximation of the conditions found on a ferry's parking deck. Two cars are placed behind each other and the AGV is tasked with passing underneath the vehicles in a straight line, turning around, and returning to a location near the starting point next to the vehicles.
3.2	Temperature readout and license plate detection in relevant environment	In the same parking garage setting, the AGV is placed behind the parked vehicles and tasked with reporting minimum and maximum temperatures in its field of view, as well as reporting the license plate of the vehicle ahead.
3.3	Combined navigation, temperature readout, and license plate detection in relevant environment	This task is a combination of T3.1 and 3.2.
4.1	Battery runtime test	This test consists of the AGV continuously navigating/circling between a set number of waypoints from a full battery charge until depletion to determine the maximum run time of the battery under operating conditions.

## 8.2 Test results

### T1.1 - PID motor control isolated

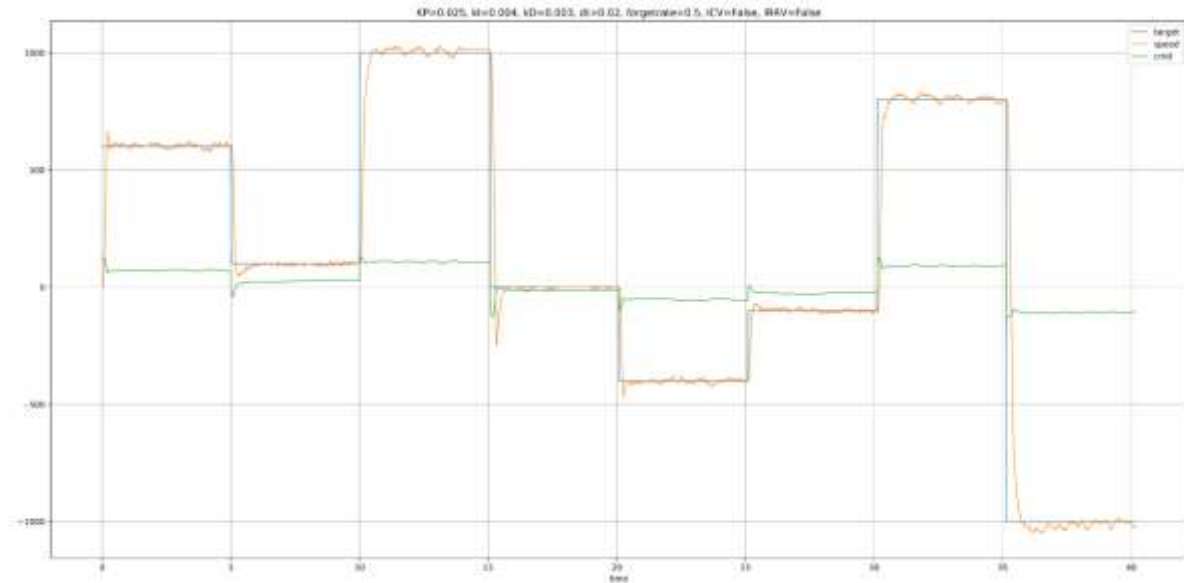


Figure 35 PID based motor control test, stepped. Blue: target speed, orange: achieved speed, green: command signal.

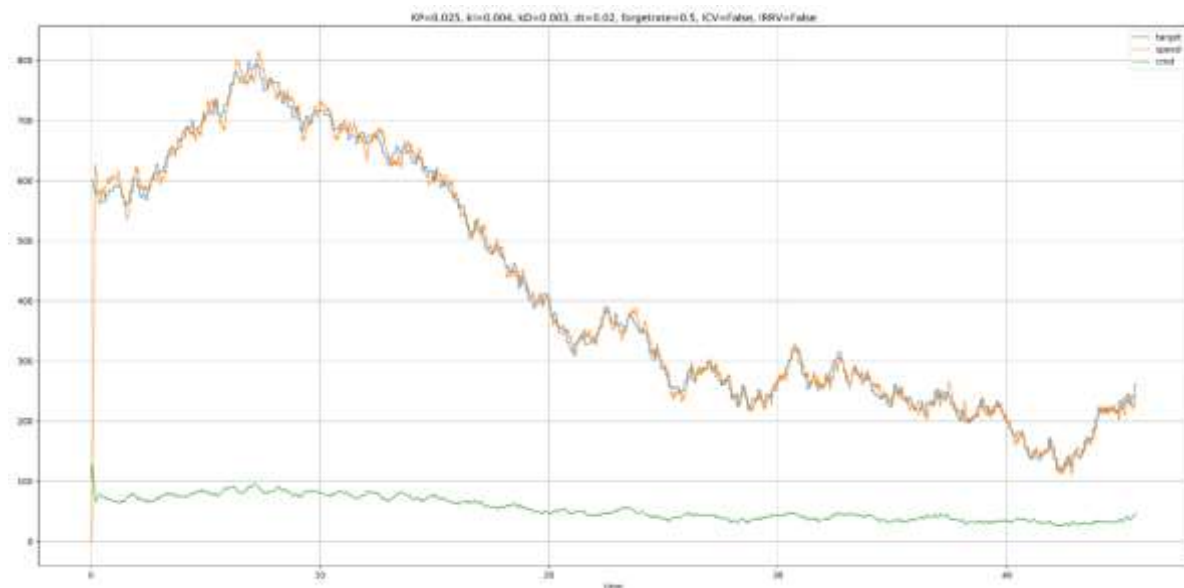


Figure 36 PID based motor control test, random. Blue: target speed, orange: achieved speed, green: command signal.

For the PID motor control test, the AGV's chassis was placed on a box to keep it stationary while the tracks spun freely. This setup is a simplification of the use case scenario but was chosen for the reproducibility of results through any number of runs. Figure 35 and Figure 36 show the test outcomes; target motor speeds (blue) were sent to the PID controller, which produces a command signal (green) such that the requested speed is enacted as precisely as possible. The measured encoder speeds (orange) follow the target closely with minimal errors in both tests, and constant speed targets are met with a near perfectly constant motor output. Thus, requirements R9.1 and R9.2 are fulfilled.



### T2.1 - Collision avoidance for dynamic obstacles (lab test)

In this test the AGV was tasked with reaching a target point. On its way towards the target point, an experimenter randomly held an obstacle (license plate) into the AGV's path, to trigger an emergency stopping. While no formal documentation was kept, the AGV stopped immediately once the object was held in front of it and continued moving towards the target point within 1-3 seconds after the object was removed from its path. The test was repeated multiple times with virtually identical results and without any obstacle collisions. Requirement R10.5 is thus met.

### T2.2 - Navigation in lab environment

This test consists of the AGV navigating a short parcours in a lab setting (office), including the navigation around a static obstacle between two waypoints. The waypoints were provided via markers in the map file, the test thus covers requirement R10.2. All other elements of this test are also present in T3.1, where a more detailed analysis was carried out. We therefore limit the documentation of this test to the corresponding [\[video recording\]](#). The successful passing of this test demonstrates that requirements R9.3, R10.2, R10.3, R10.4, R10.5 are met.

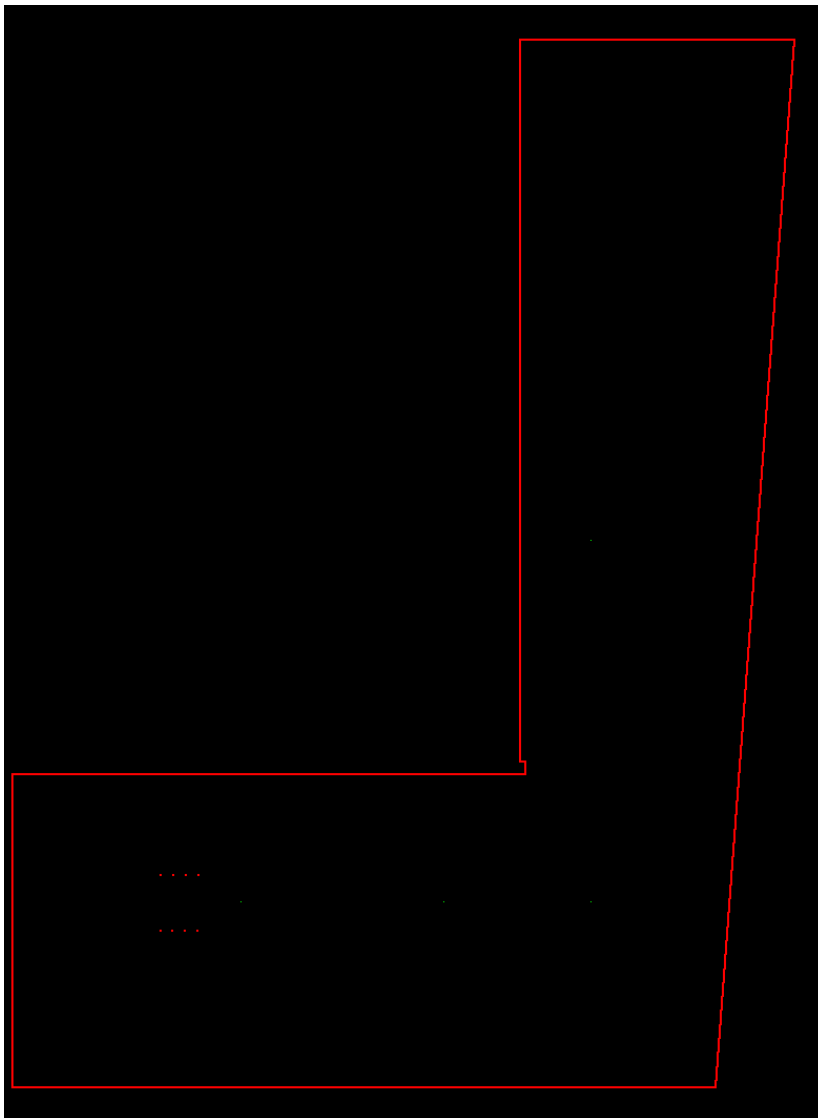


Figure 37 The static environment map used for T.2.2. Red: Solid walls and calibration rig. Green: Waypoints for map-based waypoint parsing.

### T2.3 Vehicle identification in lab environment

The license plate detection was implemented as a continuously running detection algorithm that detects whether or not a license plate is present in the frame, and in true cases it returns the detected symbols. The AGV can detect and recognize the license plates in real-time. The implementation uses a RGB camera that is plugged via USB port into the Jetson. The method called OpenALPR [16] was tested.

To test the functionalities of the license plate detection algorithms, a dataset of European license plates was used. This is to test the performance of the algorithms in a more general setting. To measure the performance two metrics are used. The first is the accuracy of how often a complete license plate has been correctly classified, that is the number of correctly read license plates divided by the total number of license plates. The second measure is the accuracy of detecting any license plate regardless of the classification being correct or not. Therefore, both the classification (detection and reading) and the detection of the license plates are evaluated.

There is a surprising lack of available license plate datasets with images of vehicles and not just the plates. While images of only plates could be useful for the classification part of the task it is also vital to be able to detect the plates in the first place. Therefore, a dataset provided by [19] was utilized as it contains a variety of images of cars with license plates in different situations. There are in total 108 images with the corresponding annotations of plate numbers. These are images taken from a variation of different vehicles, angles and slight variations in distances to the vehicles.

Larger datasets of Chinese license plates are available, but for the purposes of this study the selection was limited to European plates.

Out of the 108 images the algorithm managed to make correct classifications and detections in 78 of the cases resulting in an accuracy of roughly 72%. In 28 of the cases a license plate is detected but read incorrectly, giving an accuracy of detection alone at roughly 98%. Finally, in the remaining two cases the license plate is not detected at all. While 72% accuracy would be too low for a well performing system that causes few issues during operation it showcases the potential in this proof-of-concept. In order to increase the accuracy further larger available public datasets would be necessary, which are hard to find due to the personal information in the images.

#### Successful samples

In Figure 38 and Figure 39 two cases of correctly detected and classified plates, which read as RK715AA and RK776AI respectively by the algorithm.



Figure 38 Correctly classified vehicle by OpenALPR. Image modified from [19].



Figure 39 Correctly classified vehicle by OpenALPR. Image modified from [19].

#### Detected but incorrect samples

In Figure 40 and 41 two cases of correctly detected, but incorrectly classified plates. The plate in Figure 40 is GWAGEN, the algorithm however missed out on the W and read only GAGEN. In the case of Figure 41 the plate reads BA3020Z and the algorithm found BA3020Z. The difference is small and the "O" that is next to last was replaced with a zero. This is an error easy to make for a human as well, unless you also take into account the specific structure of the letters and numbers based on the country.



Figure 40 Correctly detected, but incorrectly classified vehicle by OpenALPR. Image modified from [19].



Figure 41 Correctly detected, but incorrectly classified vehicle by OpenALPR. Image modified from [19].

### Failed samples

In two of the cases shown in Figure 42 and Figure 43 the OpenALPR algorithm completely failed to detect a license plate.



Figure 42 Failure to detect vehicle by OpenALPR. Image modified from [19].



Figure 43 Failure to detect vehicle by OpenALPR. Image modified from [19].

### T3.1 - Navigation in relevant environment

The environment most similar to a ferry's park deck that was accessible and practical for testing was the parking garage at Lindholmen, Gothenburg. A small section of the garage was used as the test site, with two passenger EVs parked in a row. The calibration rig, i.e., the starting position for the AGV (see D08.9 [3] for details), was placed and fixated behind the parked vehicles. A map of the used section in the parking garage had been prepared, and a list of waypoints was created that would guide the AGV to pass under both vehicles before turning around and returning alongside the vehicles to a place near the starting point. Beyond text-based logs, we saved the unprocessed SLAM

maps as well as the global maps overlaid with visual markers documenting waypoints, planned paths, the AGV's past trajectory, etc.

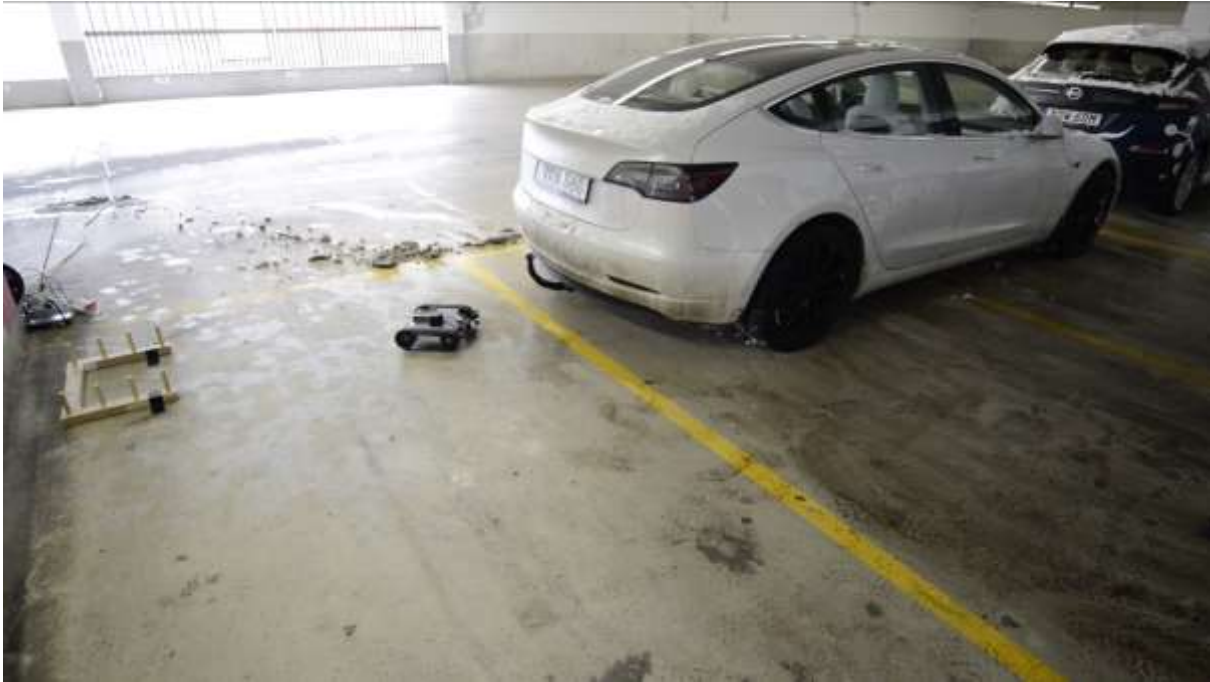


Figure 33. Test setup for tests T3.1, T3.2, and T3.3.

A [video](#) was created showing synchronized footage from two cameras and the progression of global maps (obstacle detection, tracking, path finding) for this test. The clip demonstrates the AGV's general ability to perform automated driving functions in a realistic environment with wet, dirty floor and vehicles. And low ground clearance BEVs, meeting requirement R11.1. We will now elaborate further on the meeting of module-level requirements linked to test T3.1.



Figure 44 The static environment map used for T3.1 and T3.3. It is void of waypoint markers, as these were provided via code files.



Figure 45 Unprocessed SLAM map after around 50% of the run completed.



Figure 46 Rotation aligned overlay of SLAM map (blue) and corresponding static environment map (brown). Alignment was carried out with the use of the (combined) global map.

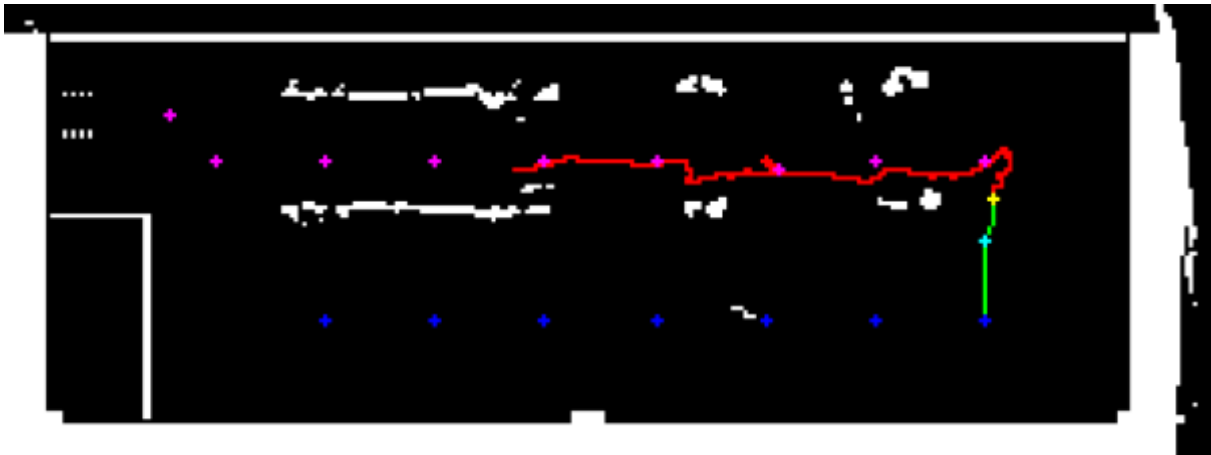


Figure 47 The global map saved by the AGV after around 50% of the run completed.

The above picture shows the global map saved by the AGV after around 50% of the run completed. For reasons of computational demand, it is downscaled in resolution by a factor of 5 compared to the static and SLAM maps and therefore more pixelated. White: Solid obstacles, either detected by the AGV's SLAM system or provided in the static environment map. Yellow: The AGV's current position. Red: The AGV's most recent trajectory. Green: The currently planned path. Turquoise: The current target waypoint. Blue: Future waypoints. Pink: Past (reached) waypoints: Red cross-markers: Skipped waypoints (these were unreachable due to obstacle proximity and were therefore progressively shifted to the nearest reachable location).

Figure 44 shows the static environment map used for tests T3.1 and T3.3. Note that additional "imaginary" walls were placed in the map to prevent the AGV from leaving the defined area at the top, or entering the area designated for test-equipment and engineers (lower left).

Figure 45 shows the unprocessed SLAM map after completing around 50% of the run. Defined outlines for the surrounding walls are visible, as are the two vehicles. However, both vehicles show accumulated evidence for the existence of obstacles in places other than the wheels. This issue occurs solely but reliably in vertically confined spaces and is related to the LiDAR's slightly upward tilt angle; the [YDLIDAR G4 specification](#) indicates 0.25° to 1.75°. Per meter distance from the LiDAR, a 1.75° upwards tilt angle would result in a 3.1cm upward shift for the laser beam, leading to the potential detection of overhead obstacles for all distances greater than about one meter away from the LiDAR. We therefore consider requirement R8.2, the creation of a sufficiently accurate SLAM map, to be only marginally met and discuss this issue further in D08.11.

Figure 46 is a manually created overlay of the unprocessed SLAM map (Figure 19) and the static environment map (Figure 18). The basis for the manual matching of the two maps was the global map saved by the AGV during the run; it is therefore an accurate recreation of the map-matching happening in the map fusion module.

The overlay shows the scaling between the two maps to be sufficiently close (R8.3 met), although slight improvements could still be made. Aside from a minor mismatch in scaling, the two maps are very precisely matched (R8.4 met): The rotation is closely matched, as evident from the alignment of the bottom wall, and the translational offset around the location of the calibration rig (top left) appears to be minimal. The correct merging of static and SLAM maps (R8.5) is, therefore, also met.

We further consider requirement R8.6 (AGV tracking accuracy within the map) to be met, as the SLAM maps created via inside-out map building are limited in accuracy by the tracking accuracy of



the AGV. In other words, if the AGV's tracking on the map were inaccurate, the created maps would be too. Since they are very precise aside from their scaling, the AGV's position within them is too. Thusly, the [\[video\]](#) also shows the AGV's tracked trajectory to match the real-world trajectory very well.

The global map, shown in Figure 47, is the outcome of the map fusion module on the AGV; an on-the-fly combination of static map and SLAM map -- thresholded, downscaled, and enhanced with relevant markers. The successful loading of the static map (R8.1) follows from its inclusion in the global map, as does the successful loading of waypoints from a list (R10.1).

Requirement R10.3 demands that an appropriate path to the next waypoint is found. This is the case, as can be seen in Figure 47 as well as the [\[video\]](#). Note that to achieve smoother operation, the path from any current waypoint A to the following waypoint B is also already computed as soon as the AGV is within a defined distance from A. Note also that the "phantom obstacles", detected due to the upward tilt angle of the LiDAR system, occasionally block the straight-line path between the AGV and the next waypoint. As intended in those cases, the path planning algorithm creates a path around the detected obstacles.

Finally, the meeting of requirements R9.3 and R10.4 -- the creation of appropriate forward velocity and angular velocity commands, as well as their sufficiently accurate enactment -- follows from the successful reaching of all waypoints. However, additional fine tuning of parameters in the forward and angular velocity command generation might yield smoother operation of the drone.

### T3.2 - Temperature readout and license plate detection in relevant environment

This test was conducted in the same environment as T3.1, with the drone statically placed behind the vehicles and inside the calibration rig (see Figure 48). The readout and logging procedure for temperatures and license plates were activated. The log file outputs show repeated readouts such as the following:

```
minTemp = -3.85 C
maxTemp = 7.97 C
detection: RkW36G
```

While we did not have any way of formally confirming the temperature readouts, they are highly plausible given ambient temperatures of around -4°C (according to The Weather Channel) at the time of testing. The license plate readout was found to be functional albeit somewhat inconsistent; in a significant fraction of repeated reads, it was recognized as "RkW6G", thus missing the "3", despite the favourable viewing angle and occlusion-free line of sight. We thus consider requirement R11.2 as

partially met.



Figure 48 Setup for isolated readouts of temperatures and license plate (T3.2).

### T3.3 - Combined navigation, temperature readout, and license plate detection in relevant environment

This test consisted of the combination of T3.1 and T3.2, i.e., the simultaneous running of the automated driving functions, and license plate and temperature readouts, and was carried out in the same environment as T3.1 and T3.2.

Unfortunately, the AGV's behaviour was found to be inadequate and partially erratic. The reason for this behaviour was determined to be exceedingly long compute times for individual modules in the automated driving functions, which may have been caused by the simultaneous running of automated driving functions and license plate detection, and their competition for compute resources. Significantly extended compute times lead to a desynchronization between the tracking and pathfinding and the real-world position and orientation of the AGV, resulting in generated commands that no longer fit its current pose. Requirement R3.3 was thus failed, and approaches to overcome this issue can be found in the discussion section.

### T4.1 - Battery runtime test

This test was planned to have the AGV perform a continuous driving task in an endless loop until the batteries are depleted. However, the chosen LiPo batteries proved highly susceptible to low charging states, i.e., once a certain low voltage level is reached, they lose their ability to be recharged and are effectively dead. This happened numerous times during the development process of the AGV, and the planned test would have most likely resulted in another lost battery. Instead, we opted for a theoretical assessment of the battery time, focused on the battery powering the main compute device and connected sensors, as it was found to be the quicker to deplete battery.

The Nvidia Jetson AGX Xavier ran in a 15W mode for the APU, and an estimated board draw of ca. 20W (due to chipset, ram, I/O controllers, and power converters). We estimate the connected sensors and WiFi antenna to consume another 10W, resulting in an estimated system power draw of around 30W. The batteries used were rated at 5200 mAh for the voltage range from 12.6V to 9V. However, without a battery management system (BMS) in place the individual cells are not depleted at the same rate, and we had to limit the used voltage range to a minimum of about 10.8V to avoid damage to the batteries. This leaves only 2600 mAh, or 29 Wh at 11.1V, the theoretical estimate of battery run time is thus 58 minutes. With that, we count the requirement R13.1 as technically fulfilled. However, as discussed in document D08.11, a switch to a different battery type, such as lithium ion, together with a BMS would be highly desirable for real world use of the AGV.

## 9 Discussion

Further ways of improving the solution and requirements to adapt it to regular operation on a ship.

### 9.1 VHD

An alternative configuration of the downward facing LWIR would be to have two LWIRs placed on each side and facing down with an angle towards the centreline. This would probably increase the line of sight and could increase the precision of the system e.g. better segmentation, cover more of the refrigeration units sides and redundancy if one sensor malfunctions or is blocked/obscured.

A connector from VHD to Terminal Operation System (TOS) and/or the shipping lines booking system, would allow a connection between the information in the booking system and the cargo/vehicle passing the gate. If information about the booked vehicle/goods is present. *Also*, a future functionality could be the verification of the object as it passes the gate in terms of size, if it is ADR/IMDG goods with signs/placards visible or missing, and by the shape if the ML is trained for such features. If the system at the terminal is made up by two portals, a database that keep track of the individual units and their measurements over time e.g. one at the entrance to the terminal and the second prior to loading on to the ship even more knowledge about the vehicles would be achieved.

### 9.2 License plate detection

A system like the LF VHD system with the capabilities to identify both truck and trailer individually and ADR/IMDG placards. This opens up for a system of systems concept, where data from VHD system can be matched with data in the booking system. This could help identifying missing ADR/IMDG placard, it also allows the terminal operator to keep track of units that have failed to comply with ADR/IMDG standards and other data such as heat signature of components on the truck and trailer. This information could be shared with the driver about their units and hopefully lead to increased awareness and standard on the units. The information about the units could also be shared with other terminals, mitigating sub-standard units from other routes and thereby forcing a good standard on the units.

A VHD system is well suited for screening a large amount of vehicles/cargo. The modifications made for this project shows that adding a top-down facing LWIR can capture the heat signature from the refrigeration unit. There are challenges for the system as such and design/placement decisions that must be considered by ship/terminal owner/operators.

In this project it has been demonstrated that a single LWIR sensor in conjunction with the side LWIR sensors can capture a lot of information about the temperature status of the refrigeration unit without intrusion or slowing down the flow of vehicle/units coming into the terminal.

## Refrigeration units

By design they are well insulated, and an increasing internal temperature due to a malfunction will have to propagate to the surface of the cowling that covers the mechanical and electrical components inside before an external sensor like a LWIR sensor can detect it at the surface.

## Aerodynamics and sound suppression barriers

The refrigeration unit are often hard to see clearly from all sides with remote sensing system. This is especially true from the front of the refrigeration unit, which is often in a narrow void between the back of the trucks cabin and the front of the trailer. Making the task for the sensors even harder there are often aerodynamical spoilers and sound barriers in place, blocking much of the free line of sight for the sensors.

## Location of the VHD system

At Stena Line's terminal at Majnabbe in Göteborg, the system was installed at the gate where Stena Line already had infrastructure for automatic documentation of incoming units using cameras. Even if the gate was designed for that system modifications were needed both to the VHD system by adding sensors, and the physical location, to give the VHD system as good line of sight as possible. Inside the gate house, the sensors had a good operational environment but being located close to the shoreline (approximately 200m from the quay side) harsh weather had an impact on the systems performance. Locating the system closer to the ramps leading to the ships, could expose the system to harsh weather conditions. Also, the flow of the departing units and the units to be loaded is usually a flexible solution where the rolling units can manoeuvre freely with as few obstacles as possible. A VHD system requires the flow to be harmonised and the sensors need free line of sight and some variations in distance and angle can be tolerated but to perform the object should be within a certain area/position. This will have implications for the loading operations in many terminals.

## Normal operation temperature baseline on refrigeration units

Data collected indicates a large spread, and the number of outliers above 124° Celsius is 68. So, it should be fair to say that it is normal with at least 124° Celsius but how much higher this study cannot answer. LASHFIRE proposed a specific project that has the goal of determining this, since it would most probably require specially designed tests where different types/manufacturers refrigeration are exposed to high workloads running on both combustion engine and electrical motors, pushed to the point where components fail or overheat, and an ignition of material/components is documented. This types tests should be of interest for authorities, road, rail and air cargo as for shipping lines, manufacturers and the fire safety industries.

## 9.3 AGV

### LiDAR

With regards to navigation capabilities, an important limitation of the AGV solution developed in this project is connected to the LiDAR system in use, i.e., the YDLIDAR G4. The task of navigating a ground vehicle underneath passenger and freight vehicles requires an accurate mapping of the environment in vertically confined spaces. This in turn requires the vertical tilt angle of the 2D LiDAR system to be as close to 0 as possible, also referred to as a flat scan field. When the scan field is not flat objects such as a car's floor or outer bodywork may be detected as obstacles, despite there being sufficient ground clearance for the AGV to pass underneath. The tilt angle depends on manufacturing precision and tolerances, and some manufacturers may opt for a slight upward tilt angle bias to avoid detecting the ground as an obstacle. Moreover, as navigation in vertically confined spaces is a rather

niche requirement in the field of robotics, the vertical tilt angle range is often omitted from spec sheets.

The prototype used the YDLIDAR G4 [20], which specifies an average tilt angle of  $1^\circ$ , and  $0.25^\circ$  and  $1.75^\circ$  as minimum and maximum tilt angle respectively, with our estimates for the unit used in this project getting closer to the upper end of that range. For reference, a  $1^\circ$  vertical tilt angle will result in a vertical offset of ca. 1.7cm per meter distance, and a  $1.5^\circ$  vertical tilt angle will result in a 7.9cm vertical offset at a distance of just 3 meters. This explains the tendency of our AGV to detect “phantom obstacles” underneath vehicles, and to detect more distant vehicles in their entirety as solid obstacles, rather than just detecting their wheels as obstacles.

To mitigate or eradicate this issue, a different LiDAR system with lower vertical angle margins and ideally no upward tilt angle bias should be sourced. The YDLIDAR TG15 [21, TG30 [22], and TG50 [23] systems each specify tilt angles between 0 and 1 degrees, which is preferable over the G4, but may still require manual testing of several units to find one with a low enough vertical tilt. The Scantec A3M1 specifies a scan field flatness of  $\pm 1.5^\circ$  and thus appears to have no upward tilt angle bias, but rather high tolerances, and it too would likely require manual testing and selection of the best unit or units. Sourcing the right LiDAR solution may thus require direct communication with manufacturers who do not specify tilt angles / scan field flatness.

Alternatively, a 3D LiDAR scanner such as the Yujin YRL3V2 [24] with a 3D SLAM system would solve this problem trivially, but a 3D SLAM system would most likely come with significantly higher compute overhead, making 2D solutions the preferred choice. It could however be explored whether or not a given 3D LiDAR scanner could be run in a 2D mode at a manually selected vertical tilt angle, or whether individual 2D-layers can be isolated from the 3D data output in order to run a 2D SLAM system.

Overall, the sourcing of a suitable LiDAR solution should be given high priority in the conceptualization of an upgraded AGV.

### Computer Hardware

The automated navigation and locomotion systems as described in 7.3.3 are compute-intensive and the update-rate of the navigation system is dependent on the available compute resources. More frequent updates, and a reduction of instances in which extended compute times disrupt the 5Hz update cycle would make the automated driving functions more robust and less error prone. While this may be partially achieved by software optimisations, increased compute capacity is highly desirable.

The Nvidia Jetson Orin [25] line of devices was released in 2022 and would be a suitable platform that builds on the capabilities of the Nvidia Jetson Xavier [26] platform used on the AGV built in this project. It offers both a higher performance per CPU core, as well as up to 4 more CPU cores in total. Its 3x performance increase for AI/tensor/GPU processing would provide additional headroom to offload CPU compute tasks such as object / license plate recognition onto GPU.

Another aspect of the used compute device is its size, weight, and I/O-configuration. A more efficient placement of USB connectors could potentially negate the need for an external USB extension card as used in the current AGV. A physically smaller compute device would free up additional space, allowing for a smaller and lighter AGV and/or extended battery life. The Nvidia Jetson Orin architecture provides multiple options here as well, and in particular the Orin NX line might be considered for this purpose.

### Motor controller

The RoboClaw motor controller board [27] proved somewhat problematic, as its drivers appeared buggy, and we had to implement PID controllers for motor speed control on the main compute device (see section 5.1.6), instead of offloading this task to the motor controller board. Due to the chip shortages during 2021 and 2022, we were unable to source an alternative motor controller board in a timely manner. In an upgraded AGV however, it would be very desirable to address this issue and offload some compute overhead from the main compute device.

### Batteries

As mentioned in section 7.1.2, the usage of LiPo batteries had some drawbacks, with the main one being the risk of over-discharging the batteries. Usually, the batteries are connected to the RC vehicle which has a Battery Management System (BMS) that maintains the health of the batteries by not allowing over-discharging. In the case with the drone, there was no BMS, since one battery was connected directly to the Jetson, and one battery directly to the RoboClaw controller. Depending on the load of the system, this had the potential of increasing the current draw, which in turn drained the batteries faster, which could over-discharge the batteries due to lacking a BMS. The over-discharging of batteries can render them useless and even dangerous.

For a future system it is suggested to build a dedicated system-specific battery with an accompanying BMS to increase the maintainability and availability of the system. This can be done using LiPo or Li-ion batteries and a BMS integrated circuit, which is readily available from electrical component suppliers. However, this means that the size of the drone needs to take the size of the batteries into greater account, as there is less flexibility regarding the layout of the batteries.

An additional benefit of creating these application specific batteries, is that it will allow for the tailoring of the voltage, which means that the optimal voltage of the motor controller (and the motors) can be reached. This will in turn increase the performance and reliability of the motors (torque, max RPM, "smoothness"), and the general movement abilities of the drone.

As the drone is meant to be automated to a great extent, this means that it is desirable to charge the batteries automatically, without the need of human input. This can be accomplished through having a dedicated charging station, that the drone knows the location of, and returns home to, after each accomplished scan/survey of the area. Methods of transferring power include induction, as well as through physical connections on the drone and the charging stations. The onboard BMS would handle risks such as over-charging and over-discharging.

### Code performance optimization

As explained in 7.1.5 (compute hardware), compute times of various processes running on the main compute device have a notable impact on the automated navigation and locomotion capabilities of the AGV. While upgrading the compute hardware to a more powerful and energy-efficient platform is a logical step in the conception of an upgraded AGV, optimizations in software can often have a significantly larger effect on overall compute time of a task. For individual functions or modules, the difference between an efficient and inefficient implementation can span several orders of magnitude.

During development of the AGV the performance of the implemented code was treated with high priority, and any computationally demanding processes were thoroughly optimized. We therefore do not expect potential code optimizations to improve compute time of individual functions or modules to yield orders-of-magnitude improvements. However, a rigorous analysis of performance and compute demand should nevertheless be carried out. In particular, the distribution of compute tasks

over different processes (running on different CPU cores or threads) and the optimization of system parameters may yield significant improvements in compute time. For instance, at the time of writing of this report, parameters such as the size of the LiDAR scan field or the resolution scaling of the global navigation map were set to assert good functionality but have not been thoroughly analyzed and tested for an optimal trade-off between functionality and compute demand. For the optimized distribution of compute tasks over multiple processes on the CPU, a complete analysis of compute times per functional module and over the course of extended field runs would have to be performed, before deciding on changes to the process structure of the implemented system.

#### License plate detection

The currently used license plate detection algorithm is CPU-based, and thus competes for compute resources with the navigation and locomotion systems. Switching to a CUDA-based system would free up some compute resources on the CPU, and no competing tasks are running on CUDA-cores. This would potentially allow for higher performing detection algorithms that could also help to overcome existing issues with acute viewing angles from below or partial occlusion.

A second noteworthy point is that OpenALPR has the downside of only working for a specific type of license plates as a time, e.g., European, American, etc. In the case of a mixed vehicle pool, it would therefore struggle unless an automatic detection of the country of origin for the vehicle is first used. It has been deemed outside the scope for this project to implement such an algorithm, but as a future work it would be an interesting prospect to modify the system to either work for all types of license plates or automatically detect the country and change settings.

There are also still challenges with achieving a competent reading of license plates through the scanning with a camera from underneath the vehicles. Building on the discussion from D08.1 the position for a ground moving drone with a camera angled upwards can provide problematic photography angles for the license plate detector. Especially if the vehicles are closely packed with only a few centimeters distance in between, the steepness of the angle may make classifications of numberplates challenging. One of the methods how these issues could be alleviated would be to use an extendable robotic arm to create better reading possibilities. Another solution would also be to combine it with an aerial drone that has the possibility of scanning from other angles and in other areas, e.g., for ID tags placed in car windows.

The evaluation dataset used for the AGV is small and lacks variation in angles and light differences, which makes it a poor representation of the cargo spaces. A more exhaustive evaluation would need to consider these and cover more of the angles expected from underneath tightly packed vehicles.

#### Improved SLAM precision through odometry and IMU

In its current implementation, the AGV's SLAM system relies solely on the LiDAR input for mapping and localization. The used Cartographer software package, however, does feature support for both odometry and Inertial Measurement Unit (IMU) systems data. When provided as additional input to the SLAM, such data typically leads to more stable representations of both the environment and the AGV's position within it. In particular when orientation points within the LiDAR scan are sparse (which can happen on empty or partially empty parking decks), the localization of the AGV within the environment can shift, leading to double walls in the mapping and an offset of the waypoints, which may place them out of reach, or lead to part of the environment remaining unvisited. Therefore, odometry and IMU input to the SLAM system might help to mitigate or overcome potential issues caused by the limited detection range of LiDAR systems.

### Communication with external devices

In its current state, the AGV's primary output is a log file in which it keeps track of its current position and orientation on the global map, as well as the current minimum and maximum temperature detected by the IR camera, and the latest detected license plate. It would be desirable to implement a standing connection via WiFi to an external system, which would in turn be tasked with notifying the ferry's personnel or taking automatic action to prevent or mitigate damages.

### Thermal cameras

Firstly, the conclusion from chapter 7.1.6 is that one Lepton 3.5 thermal camera should be sufficient for most vehicles that the AGV is able to travel under, there are also options to improve the coverage further. To increase the range of width of thermal inspection two or more thermal cameras could be installed to cover the full width of the vehicle's battery at a closer distance. This setup would also serve as a source of redundancies where if one camera malfunctions or is occluded the area can still be covered by others. It does, however, increase the cost of equipment for an AGV and the complexity of software management. The number of available USB ports might however be a limiting factor for this and would have to be further examined before any additional sensors could be installed.

Secondly, In the proof-of-concept AGV it was deemed enough to be able to find out hotspots by detecting pixel values with abnormal heat. However, the system could benefit from an additional sensor fusion strategy. An issue that can occur with the current strategy is that an abnormal temperature could be registered from an object, which in fact is supposed or accepted to have a temperature that could otherwise be considered as a hazard. In this case there needs to be a combination of the information of the thermal camera and with either an RGB or depth camera capable of registering what object has the abnormal temperature.

### System of systems

How it all fits together as components in a puzzle, acting cooperatively, integrated or data exchange-system, to increase SA and reduce risk. This is the novel chapter in the report covering the overview and system of systems approach combining the automated guided vehicle, vehicle hotspot detection and synergies between them in identifications of vehicles and ignition sources.

With a LF-AGV concept risk reduction can be achieved as the cargo/vehicle arrives at the first point of scanning at the gate, at the yard of the terminal, and finally onboard the ship depending on the system(s) and configuration. At the ship, to the objects (cargo/vehicles) final positioning of on the deck and during the sea voyage. Depending on the terminal/ship operator's desire e.g., functionality, Gate to Ship to Gate coverage, the system goes from single point/note to a mesh of system of systems.



## 10 Conclusion

Main author of the chapter: Robert Rylander, RISE

Two demonstrators have been developed: a VHD gate system capable of scanning vehicles passing through located in the port at the Majnabbe terminal in Gothenburg and a mobile AGV capable of continuously scanning vehicles for heat anomalies.

The tests of both the VHD and the AGV show that each system can function independently or in concert. As stand-alone systems they can decrease fire risk by supporting personnel or stowage planning systems, providing them with greater insight into the current state of objects on the ship that have a fire risk.

The VHD system does this at a much higher efficiency, speed, and thoroughness than people would likely be able to do directly. In combination with data from the transport log this could lead to other benefits, such as improved standardization.

The AGV system minimizes fire risk by allowing for data gathering in a way not possible for personnel on a ship. By navigating under vehicles that are packed tightly in the ship's hold the AGV system supports allows for early warning and prevention. Because the AGV can do so multiple times on a voyage the system can also capture relevant information over time, which minimizes the likelihood of missed warning signs due to a snapshot, such as when the vehicle is loaded.

The greatest benefit is when these systems work in concert, not only with each other, but also with the transport log and personnel at the terminal and onboard. Integrating these multiple human and technical systems has the potential to dramatically reduce fire risk.

## 11 References

- [1] D08.1 Definition and parametrization of critical fire hazards, classification of cargoes, transport units, engines, fuels and vessels and identification methodologies May 2021  
[https://lashfire.eu/media/2021/10/LASH-FIRE\\_D08.1\\_Definition-fire-hazards-cargoes-identification\\_v06-4.pdf](https://lashfire.eu/media/2021/10/LASH-FIRE_D08.1_Definition-fire-hazards-cargoes-identification_v06-4.pdf) [Accessed March 2023]
- [2] LASH FIRE. (2020). *LASH FIRE Deliverable D04.1* Review of accident causes and hazard identification report: [https://lashfire.eu/media/2021/04/LASH-FIRE\\_D04.1\\_Review-of-accident-causes-and-hazard-identification-workshop-report.pdf](https://lashfire.eu/media/2021/04/LASH-FIRE_D04.1_Review-of-accident-causes-and-hazard-identification-workshop-report.pdf) [Accessed March 2023]
- [3] D08.9 Prototyping and demonstration of vehicle identification tool.  
<https://lashfire.eu/deliverables/>
- [4] D08.10 Demonstration of prototype for detection of potential ignition sources.  
<https://lashfire.eu/deliverables/>
- [5] D08.2 Fire hazard mapping visualization tool with fire hazard matching integrated (January 2022)  
[https://lashfire.eu/media/2022/02/LASH-FIRE\\_D08.2\\_Fire-hazard-mapping-visualization-tool-with-fire-hazard-matching-integrated.pdf](https://lashfire.eu/media/2022/02/LASH-FIRE_D08.2_Fire-hazard-mapping-visualization-tool-with-fire-hazard-matching-integrated.pdf) [Accessed March 2023]
- [6] D07.6 Alarm-system-interface-prototype-development-and-testing  
[https://lashfire.eu/media/2022/10/LASH-FIRE\\_D07.6\\_Alarm-system-interface-prototype-development-and-testing.pdf](https://lashfire.eu/media/2022/10/LASH-FIRE_D07.6_Alarm-system-interface-prototype-development-and-testing.pdf)
- [7] FLIR. (2021). FLIR. <https://www.flir.eu/products/lepton/> [Accessed: 2023-03-17]
- [8] YDLIDAR. (n.d.). YDLIDAR G4. <https://www.ydlidar.com/products/view/3.html> [Accessed: 2023-03-16]
- [9] Logitech. (2023). C930e – FÖRETAGSWEBBKAMERA. <https://www.logitech.com/sv-se/products/webcams/c930e-business-webcam.960-000972.html> [Accessed: 2023-03-17]
- [10] Nvidia. 2020. Buy the Latest Jetson Products. <https://developer.nvidia.com/buy-jetson>
- [11] FLIR. (2021). FLIR. <https://www.flir.eu/products/lepton/> [Accessed: 2023-03-17]
- [12] GroupGets. (2023). <https://groupgets.com/> [Accessed: 2023-03-14]
- [13] Blender. (n.d.). Blender. <https://www.blender.org/> [Accessed: 2023-03-17]
- [14] Google. Cartographer ROS Integration. Retrieved from Cartographer ROS: <https://google-cartographer-ros.readthedocs.io/en/latest/index.html> [Accessed: 2021-03-01]
- [15] Huiming Zhou. (2020). PathPlanning. [https://github.com/zhm-real/PathPlanning/blob/master/Search\\_based\\_Planning/Search\\_2D/Astar.py](https://github.com/zhm-real/PathPlanning/blob/master/Search_based_Planning/Search_2D/Astar.py) [Accessed: 2023-03-16]
- [16] OpenALPR. (2020). openalpr. <https://github.com/openalpr/openalpr> [Accessed: 2023-03-15]
- [17] GroupGets. (2016). Libuvc. [GitHub - groupgets/libuvc: a cross-platform library for USB video devices](https://github.com/groupgets/libuvc) [Accessed: 2023-03-14]
- [18] GroupGets. (2019). PureThermal UVC Capture Examples. [GitHub - groupgets/purethermal1-uvc-capture: USB Video Class capture examples for PureThermal 1 / PureThermal 2 FLIR Lepton Dev Kit](https://github.com/groupgets/purethermal1-uvc-capture) [Accessed: 2023-03-15]

- [19] OpenALPR, 2017. Benchmarks. Available at: <https://github.com/openalpr/benchmarks> [Accessed 2023-03-14].
- [20] YDLIDAR. (n.d.). YDLIDAR G4. <https://www.ydlidar.com/products/view/3.html>  
[Accessed: 2023-06-19]
- [21] YDLIDAR. (n.d.). YDLIDAR TG15. <https://www.ydlidar.com/products/view/16.html> [Accessed: 2023-03-16]
- [22] YDLIDAR. (n.d.). YDLIDAR TG30. <https://www.ydlidar.com/products/view/14.html> [Accessed: 2023-03-16]
- [23] YDLIDAR. (n.d.). YDLIDAR TG50. <https://www.ydlidar.com/products/view/19.html> [Accessed: 2023-03-16]
- [24] Yujinrobot. (n.d.). Yujin 3D LiDAR. [http://lidar.yujinrobot.com/?page\\_id=10&ckattempt=1](http://lidar.yujinrobot.com/?page_id=10&ckattempt=1)  
[Accessed: 2023-03-16]
- [25] NVIDIA. (2023). NVIDIA Jetson Orin NX 16GB Module. <https://www.nvidia.com/en-us/autonomous-machines/embedded-systems/jetson-orin/> [Accessed: 2023-03-16]
- [26] Nvidia. (n.d.). *Jetson Xavier NX*. Retrieved from <https://developer.nvidia.com/embedded/jetson-xavier-nx>
- [27] NVIDIA. (n.d.). RoboClaw 2x15A Motor Controller. [https://www.basicmicro.com/RoboClaw-2x15A-Motor-Controller\\_p\\_10.html](https://www.basicmicro.com/RoboClaw-2x15A-Motor-Controller_p_10.html) [Accessed: 2023-03-16]

## 12 Indexes

### 12.1 Index of tables

Table 1 Example of temperature thresholds used in road tunnels.....	13
Table 2 New requirements on the VHD system.....	14
Table 3 New functionality in the VHD system.....	14
Table 4 New functionality in the VHD system.....	19
Table 5 Temperature of the top six refrigeration units captured in the data set (Celsius). ....	34
Table 6 AGV Functional requirements. ....	53
Table 7 AGV Test scenarios. ....	54

### 12.2 Index of figures

Figure 1 Illustration of the physical installation of a VHD system (SICK) .....	12
Figure 2 The two LiDARs used for longitudinal tracking of the object. (SICK) .....	12
Figure 3 Segmentation of sections of interest by the software in VHD system (SICK) .....	13
Figure 4 The principle for ANPR (SICK) .....	22
Figure 5 The ANPR cameras reading the rear of the vehicle. (STL).....	22
Figure 6 Front ANPR cameras, facing south in the gate house. (STL) .....	23
Figure 7 Side view of front ANPRs. (STL) .....	23
Figure 8 Screen showing a ADR/IMDG marked IBC.....	24
Figure 9 Truck and trailers license plates are read and presented to the operator via TEMS Analyzer user interface. ....	25
Figure 10 Overheated brakes on trailer with ADR/DG goods. ....	25
Figure 11 Rear of the trailer showing signs and placards. ....	26
Figure 12 ADR/DG number 2280 placard singled out. ....	26
Figure 13 ADR/DG placard visible via CCTV.....	26
Figure 14 Forward positioning LiDAR at Majnabbe. (STL).....	28
Figure 15 Rear LiDAR for positioning and tracking of vehicle. (STL) .....	29
Figure 16 LiDAR and LWIR for right side of the vehicle. (RISE) .....	30
Figure 17 Sensor array including the ambient temperature sensor. (RISE) .....	31
Figure 18 LiDAR and LWIR for left side of the vehicle. (RISE)i.....	31
Figure 19 Reefer hotspot highlighted in TEMS SW .....	32
Figure 20 Segmentation of refrigeration unit based on machine learning presented in 2D and 3D....	32
Figure 21 Scatterplot and a trendline of temperature from refrigeration units from the top-down facing LWIR sensor. ....	33
Figure 22 All three LWIR sensors with their spread in degrees Celsius and an average of the three sensors.....	34
Figure 23 Using ML to find and segment refrigeration units on both the truck and the trailer.....	35
Figure 24 VHD Alarm is triggered.....	36
Figure 25 Dialogue with driver and is an Inspection possible to perform?.....	37
Figure 26 What action should be taken? .....	38
Figure 27 Render of the final version of the AGV .....	39
Figure 28 Coverage of a typical passenger vehicle's battery with the IR camera.....	43
Figure 29 Render of the AGV's final internal component layout. ....	44
Figure 30 Renders of the custom hardware pieces on the AGV. ....	45
Figure 31 Render of an earlier version of the AGV with a visual depiction of the IR camera's field of view. ....	45
Figure 32 Conceptual sketch of processing flow (sense-plan-act control architecture, license plate detection and thermal imaging).....	47

Figure 33 Top: static environment map, middle: dynamic SLAM map (unprocessed), bottom: global map..... 49

Figure 34 Render of the AGV placed in the calibration rig..... 50

Figure 35 PID based motor control test, stepped. Blue: target speed, orange: achieved speed, green: command signal. .... 55

Figure 36 PID based motor control test, random. Blue: target speed, orange: achieved speed, green: command signal. .... 55

Figure 37 The static environment map used for T.2.2. Red: Solid walls and calibration rig. Green: Waypoints for map-based waypoint parsing. .... 56

Figure 38 Correctly classified vehicle by OpenALPR. Image modified from [19]. .... 58

Figure 39 Correctly classified vehicle by OpenALPR. Image modified from [19]. .... 58

Figure 40 Correctly detected, but incorrectly classified vehicle by OpenALPR. Image modified from [19]. .... 59

Figure 41 Correctly detected, but incorrectly classified vehicle by OpenALPR. Image modified from [19]. .... 59

Figure 42 Failure to detect vehicle by OpenALPR. Image modified from [19]..... 60

Figure 43 Failure to detect vehicle by OpenALPR. Image modified from [19]..... 60

Figure 44 The static environment map used for T3.1 and T3.3. It is void of waypoint markers, as these were provided via code files..... 61

Figure 45 Unprocessed SLAM map after around 50% of the run completed. .... 62

Figure 46 Rotation aligned overlay of SLAM map (blue) and corresponding static environment map (brown). Alignment was carried out with the use of the (combined) global map..... 62

Figure 47 The global map saved by the AGV after around 50% of the run completed. .... 63

Figure 48 Setup for isolated readouts of temperatures and license plate (T3.2). .... 65

## 13 ANNEXES

### 13.1 ANNEX A Highest 100 recorded refrigeration units

The highest one hundred refrigeration units, three thermal sensors and an average of these three in Celsius.

Top 100	Right	Top	Left	Average*
1	58,4	225,7	79,7	121
2	30,1	214,5	39,1	95
3	62,3	201	68	110
4	43	195,9	73,4	104
5	44,6	192,3	52,8	97
6	67,3	192,3	41,4	100
7	59,4	184,5	61,3	102
8	125,8	183,6	108,4	139
9	44,5	182,5	51,2	93
10	69,5	181,8	37,1	96
11	55,9	179,2	58,8	98
12	66,9	178,7	43	96
13	74,9	178,6	39,1	98
14	43,8	178,4	54,7	92
15	67,6	177,2	37,1	94
16	64,5	173,6	39,7	93
17	42,3	171,7	55,9	90
18	68,1	171,5	41,5	94
19	55,2	171,2	59,4	95
20	57,6	168,5	41,6	89
21	111,5	164,5	55,7	111
22	40,7	164,2	50,9	85
23	51,6	164,2	48,3	88
24	54,1	164	59,2	92
25	47,1	160,8	39,6	83
26	46,7	160,4	51,5	86
27	53,7	159,6	42,9	85
28	54,1	158,9	57,5	90
29	49,7	158,8	56,2	88
30	38,7	157,6	47,9	81
31	42,4	157,6	41,7	81
32	52,8	156	49,8	86
33	56,1	155,8	48,3	87
34	50,2	151,6	56,8	86
35	63	150,7	39,1	84
36	94,9	150,7	98,3	115
37	62,1	150,6	48,7	87
38	50,3	149,4	42,9	81
39	53,2	148,8	77	93
40	54,9	148,4	39,4	81
41	43,4	148,3	58,5	83
42	47,5	148	48,9	81

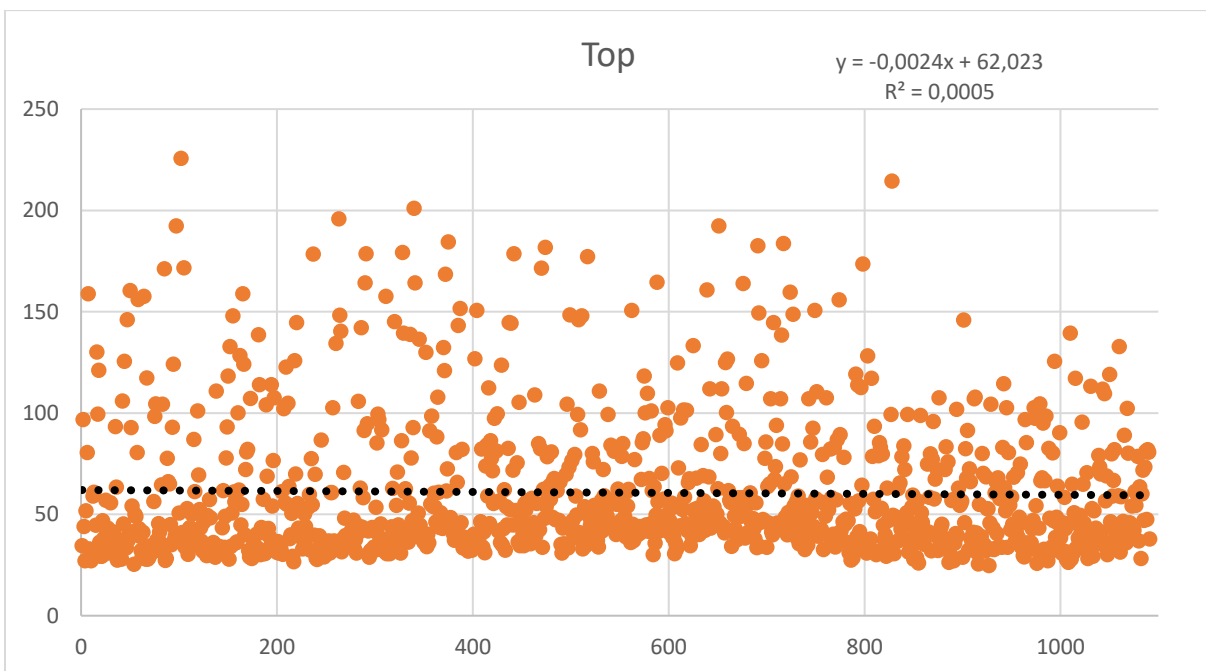
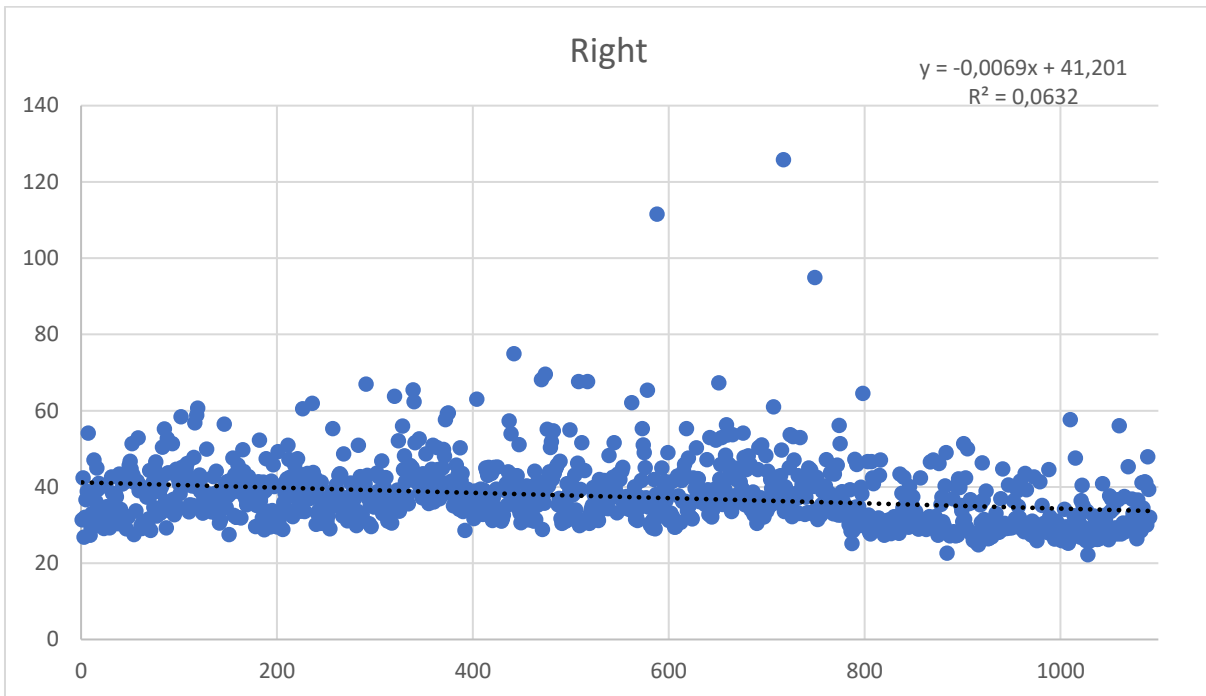
43	51,6	147,9	40,2	80
44	41,5	146,1	117,5	102
45	67,6	146,1	40,1	85
46	51,3	146	92,3	97
47	63,7	145,2	39,5	83
48	41,7	144,7	53,6	80
49	57,3	144,7	46,7	83
50	61	144,7	37,8	81
51	53,9	144,3	40,5	80
52	43,3	143,3	47,7	78
53	40	142,1	49,7	77
54	43,1	140,4	47,9	77
55	44,5	139,5	43,9	76
56	57,6	139,4	40,9	79
57	45,6	138,8	74,8	86
58	41,3	138,7	37,5	73
59	49,6	138,5	39,3	76
60	52,6	136,4	53,2	81
61	40,4	134,4	58,1	78
62	42,3	133,3	46,9	74
63	41,7	132,8	46,8	74
64	56	132,8	42,5	77
65	49,8	132,3	48,9	77
66	44,9	130,2	50,8	75
67	48,6	129,9	46,1	75
68	38,6	128,4	45,3	71
69	46,6	128,2	39	71
70	38,9	126,8	37,9	68
71	53,6	126,7	43,2	75
72	45,7	125,9	46,4	73
73	51	125,8	40,9	73
74	41,6	125,6	48,9	72
75	26,3	125,5	28,5	60
76	48,3	124,9	44,5	73
77	42,8	124,7	43,7	70
78	44	124,2	48,9	72
79	36,7	124,1	41	67
80	31	123,7	32,1	62
81	41,4	122,7	49,1	71
82	40,9	121,1	39,4	67
83	48	121	54,8	75
84	34,7	119,2	74,6	76
85	37,6	119	38,6	65
86	37,6	118,3	40	65
87	49	118,3	39,2	69
88	37,3	117,3	66,9	74
89	46,6	117,2	37,9	67
90	47,5	117,1	44,6	70

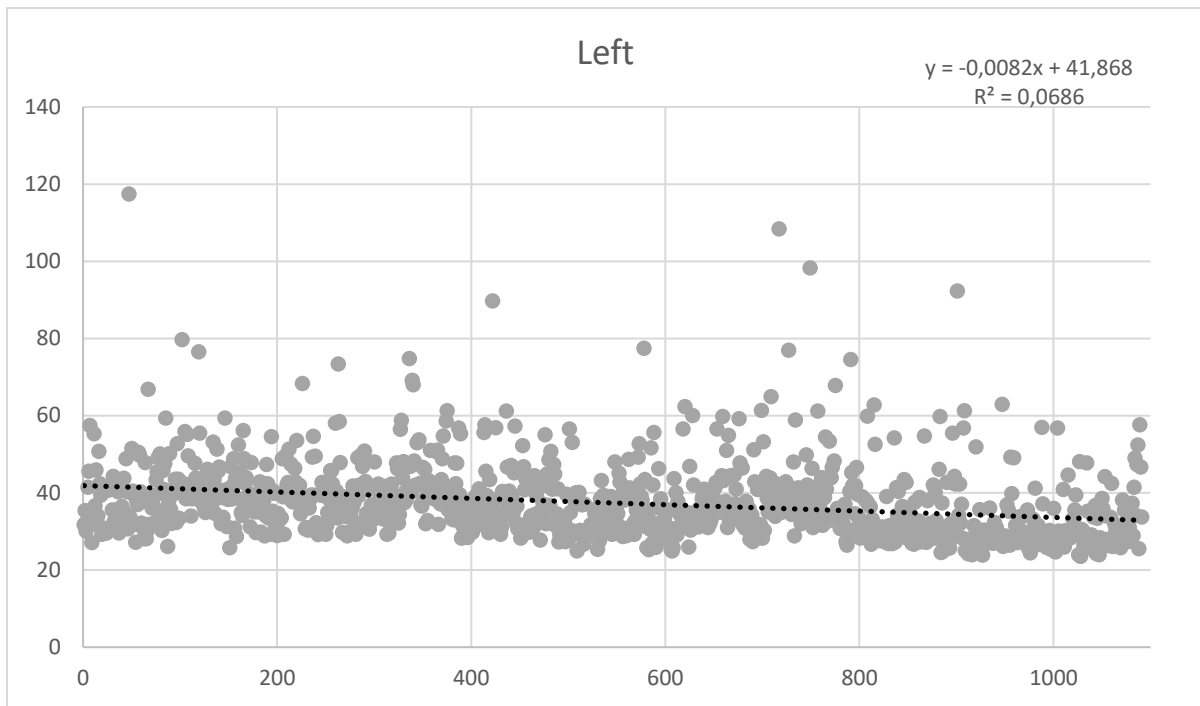
91	44,5	114,6	46,5	69
92	29	114,5	28,4	57
93	52,2	114	42,9	70
94	41,5	114	54,6	70
95	32	113,9	41,9	63
96	26,1	113,2	26,3	55
97	39,9	112,6	41,9	65
98	45,1	112,4	39,3	66
99	52,9	112	40,7	69
100	52,9	112	42,7	69



### 13.2 ANNEX B Plots of LWIR temperature readings

Plots from the LWIR sensors reading Right side, Top down and Left side.





### 13.3 ANNEX C Most used temperature settings in VHD systems

The most used temperature setting used in VHD systems.

	Car Or Van	Truck	Bus
Contour	460	460	460
Wheel	120	90	70
Load	80	120	80
Passenger	80	80	80
Engine	350	500	350
RefrigerationUnit	TBD*	TBD*	TBD*
Reflection	350	500	350
BreakDisc	150	120	120

\*TBD- To Be Determined